© Copyright 2004
Audrey Seamons

Implications of Myelin Basic Protein Processing and Presentation on T Cell Activation and Tolerance

Audrey Seamons

A dissertation
submitted in partial fulfillment of the
requirements for the degree of

Doctor of Philosophy

University of Washington

2004

Program Authorized to Offer Degree:
Genome Sciences--Molecular Biotechnology

UMI Number: 3118869

Copyright 2004 by
Seamons, Audrey

All rights reserved.

INFORMATION TO USERS

The quality of this reproduction is dependent upon the quality of the copy submitted. Broken or indistinct print, colored or poor quality illustrations and photographs, print bleed-through, substandard margins, and improper alignment can adversely affect reproduction.

In the unlikely event that the author did not send a complete manuscript and there are missing pages, these will be noted. Also, if unauthorized copyright material had to be removed, a note will indicate the deletion.

UMI®

UMI Microform 3118869
Copyright 2004 by ProQuest Information and Learning Company.
All rights reserved. This microform edition is protected against unauthorized copying under Title 17, United States Code.

ProQuest Information and Learning Company
300 North Zeeb Road
P.O. Box 1346
Ann Arbor, MI 48106-1346

University of Washington
Graduate School

This is to certify that I have examined this copy of a doctoral dissertation by

Audrey Seamons

and have found that it is complete and satisfactory in all respects,
and that any and all revisions required by the final
examining committee have been made.

Chair of Supervisory Committee:

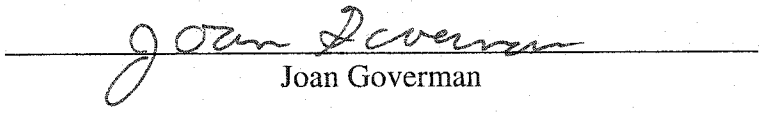

Joan Goverman

Reading Committee:

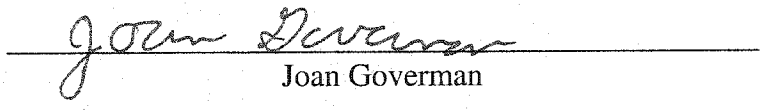

Joan Goverman

Craig Beeson

Alexander Rudensky

Date: March 8, 2004

In presenting this dissertation in partial fulfillment of the requirements for the doctoral degree at the University of Washington, I agree that the Library shall make its copies freely available for inspection. I further agree that extensive copying of the dissertation is allowable only for scholarly purposes, consistent with "fair use" as prescribed in the U.S. Copyright Law. Requests for copying or reproduction of this dissertation may be referred to Proquest Information and Learning, 300 North Zeeb Road, Ann Arbor, MI 48106-1346, to whom the author has granted "the right to reproduce and sell (a) copies of the manuscript in microform and/or (b) printed copies of the manuscript made from microform."

Signature Audrey Seamon

Date March 8, 2004

University of Washington

Abstract

Implications of Myelin Basic Protein Processing and Presentation on T Cell Activation and Tolerance

Audrey Seamons

Chair of Supervisory Committee:
Associate Professor Joan Goverman
Immunology

Experimental autoimmune encephalomyelitis (EAE) is an animal model for multiple sclerosis which can be induced by immunization with myelin antigens such as myelin basic protein (MBP). Immune tolerance influences the repertoire of MBP-specific T cells in B10.PL mice. MBPAc1-11-specific T cells escape tolerance while MBP121-150-specific T cells undergo tolerance *in vivo*. This differential tolerance induction may reflect unstable binding of MBPAc1-11 to I-A^u compared to stable binding of peptides within MBP121-150.

To determine which MBP epitopes are naturally processed from whole MBP, peptides eluted from I-A^u isolated from MBP-pulsed splenocytes were analyzed by mass spectrometry. Two nested sets of peptides were found, N-terminal MBP peptides and peptides containing MBP125-135. N-terminal peptides MBPAc1-18 and MBPAc1-17 were the most abundant peptides processed from whole MBP. Our investigations indicate that MBPAc1-18 can bind in the register that presents MBPAc1-11, however, most MBPAc1-18 binds in a more stable register, MBP5-16, allowing MBPAc1-11-specific T cells to escape tolerance. Additionally, endogenously derived MBP peptides are constitutively presented by B cells and dendritic cells (DCs) which are able to stimulate activated MBP121-150-specific T cells. However, only DCs are able to stimulate naïve MBP121-150-specific T cells, implicating DCs as the antigen presenting cell involved in the maintenance of peripheral tolerance to MBP.

To investigate why two different MBPAc1-11-specific T cell receptor transgenic mouse lines exhibit differences in spontaneous EAE incidence, T cell responses to MBP were compared between the two lines. While differences in T cell proliferative responses were not detected, T cells isolated from the Tg line with lower spontaneous EAE incidence did not produce IFN-γ and lower percentages of T cells produced cytokines compared to the line with higher incidence of spontaneous EAE.

We also analyzed the structural basis for cross-reactivity exhibited by T cells recognizing two distinct epitopes within MBP121-150. Mutational analysis of the CDR1 and 3 regions of one cross-reactive T cell receptor indicated that the same amino acids within CDR1 and 3 are used to recognize both epitopes.

Table of Contents

List of Figures

List of Tables

List of Acronyms and Abbreviations

MHC; major histocompatibility complex
CNS; central nervous system
MS; multiple sclerosis
EAE; experimental allergic encephalomyelitis
MBP; myelin basic protein
PLP; proteolipid protein
MOG; myelin oligodendrocyte protein
APC; antigen presenting cell
TCR; T cell receptor
Tg; transgenic
CDR; complementarity determining region
pMHC; peptide/MHC
scTCR; single chain T cell receptor
ce; cell equivalents
FT-ICR-MS; Fourier transform ion cyclotron resonance mass spectrometry
CAD; collision associated dissociation
DC; dendritic cell
Tg1; MBPAc1-11-specific TCR transgenic mouse line 1 (Vα2.3/Vβ8.2)
Tg2; MBPAc1-11-specific TCR transgenic mouse line 2 (Vα4/Vβ8.2)
BCR; B cell receptor
GALT; gut associated lymphoid tissue
SI; stimulation index
LN; lymph node
SPL; spleen
SPF; specific pathogen-free

Acknowledgements

Part of the work for this thesis was done in collaboration with Drs. Roland Strong, Craig Beeson and Donald Hunt. Daniel Morris, Vladamir Vigdorovich, Dr. Pingwei Li, Dave Goetz and Dr. Meg Holmes in Dr. Strong's laboratory helped to train me in protein expression, analysis and purification techniques. Jennifer Sutton in Dr. Hunt's laboratory performed the mass spectrometry analysis described in Chapter 4 to identify processed MBP peptides. Emily Baird, Nena Bonn and Björn Kafsack in Dr. Beeson's laboratory performed the peptide synthesis and dissociation experiments described in Chapter 4 of this thesis and also taught me how to do HPLC. The Goverman lab has been a great place to work. Antoine Perchellet, Sarah Cabbage, Ingunn Stromnes and Dr. Thea Brabb had excellent ideas and comments regarding my experimental design and interpretation and were very helpful to me by reading drafts of papers, posters and this thesis. Neal Mausolf and Molly Ottele were indispensable for many of my time-consuming experiments and are excellent managers of our mouse colonies. Their extremely cheerful dispositions always made it a pleasure to be in the lab. Eric Huseby spent a lot of time helping me to get started in the lab and also was helpful in experimental design of the mutagenesis project. Dr. Joan Goverman is an excellent mentor. She is approachable, open minded about research ideas and allows independent work. Her skills as a writer and teacher helped me tremendously and I would not have been able to finish this thesis work without her support. Lastly, I would not be at this point in my life without the support of friends and family. I am especially grateful for my husband, Todd, for putting up with me for the past five years and supporting my decision to stay in graduate school.

Dedication

I dedicate this work to my parents, Alan and Patricia Stephens, for encouraging me to continue my education and for their support of my husband and me throughout our graduate school experience.

Chapter 1: Background

Adaptive Immune System and Autoimmunity

T and B cells are the principal effector cells of the adaptive immune system. B cells have receptors that bind to soluble antigens while T cells have receptors that recognize peptides on the surface of major histocompatability complexes (MHC). The antigen binding receptor is divided into a variable domain that binds antigen and a constant domain. The variable domains of T and B cell receptors are generated by genomic recombination of V, D and J gene segments which are then joined to the constant region domain to generate a full receptor. This recombination results in the generation of a large repertoire of receptors with different binding specificities that have the potential to recognize any foreign antigen they encounter. However, this recombination can also generate receptors that are specific for self-antigens. To overcome the problem of self-reactive T and B cell receptors, mechanisms of immune tolerance either eliminate or inhibit the responses of autoreactive cells. Tolerance mechanisms are described in two general categories: 1) central tolerance mechanisms act in the tissue where T or B cells develop (in mammals these are the thymus and bone marrow, respectively) and 2) peripheral tolerance mechanisms act on mature T or B cells that have escaped central tolerance and are in circulation. Both central and peripheral tolerance mechanisms function to eliminate self-reactive immune cells, induce receptor editing or inhibit responses of self-reactive immune cells if they become aberrantly activated. Autoimmune disease results from a breakdown of these immune tolerance mechanisms. Such a breakdown in tolerance to antigens of the central nervous system (CNS) is believed to lead to the development of multiple sclerosis (MS).

Multiple Sclerosis

MS is an inflammatory demyelinating CNS disease with heterogeneous clinical signs and pathology (1). MS is thought to be an autoimmune disease for several reasons including the presence of lymphocytes and monocytes in CNS lesions (2), genetic

susceptibility is linked to MHC haplotype and other immune related loci (3) and it has many similarities to an animal model for autoimmune demyelination, experimental allergic encephalomyelitis (EAE), which is induced by activating myelin-specific T cells (4).

MS patients typically exhibit diverse symptoms which can include altered reflexes, spasticity, weakness, ataxia, sensory loss, extensor plantar responses and visual impairment. Manifestation of these symptoms is variable among individual patients and can follow an acute, relapsing/remitting or progressive disease course (1).

Pathologically, MS is characterized by demyelinated plaques in the white matter accompanied by perivascular infiltrates of T cells, B cells and macrophages. Lesion pathology observed in MS patients is diverse and has been categorized into four types (5). These categories were based on differences in the viability and mechanism of oligodendrocyte death (apoptotic or necrotic), the definition of lesion boundaries and location of lesions relative to veins. Lesions of all four types contain inflammatory lymphocytes and myeloid cells but Type II lesions are distinguished by the presence of IgG deposits as well as activated complement, suggesting a role for antibodies in the pathogenesis of these lesions (5). In addition to the lesion characteristics described above, astrocyte proliferation, gliotic scarring and axonal damage are seen in some patients (6). The recognition of distinct types of pathology has led to the view that multiple pathways may lead to the development of MS. These pathways could differ in the specific triggers of disease, the immune tolerance mechanisms that break down and the type of effector cells that cause the pathology (5-7). While these issues are difficult to study in humans, animal models for MS have provided insight into mechanisms that regulate the fate of immune cells capable of mediating CNS autoimmune disease.

EAE as a Model for MS

One of the most widely used animal models for the study of MS is experimental allergic encephalomyelitis (EAE). EAE is induced either by immunization with myelin antigens in complete Freund's adjuvant or by adoptive transfer of myelin-specific T cells

(8). The resulting disease can have many similarities to MS but due to the large variation in disease outcomes seen among individual patients with MS, one particular model of EAE will not be representative of all aspects of the disease needed for understanding, diagnosing and treating MS. EAE in animals can be similar to particular forms of MS in lesion pathology, symptoms and disease course however, these characteristics vary depending on the immunogen, species and strain used for disease induction (9). Susceptibility to EAE differs among mouse strains and is dependent on the MHC haplotype. Other susceptibility factors that have been identified include variability in antigen expression levels, differences in abilities to express certain cytokines and differences in co-stimulation between mouse strains (10).

A primary focus in studies of EAE has been to identify the effector cells which initiate disease. These efforts initially focused on the T cell responses to the major protein components of the myelin sheath: proteolipid protein (PLP) and myelin basic protein (MBP). T cells specific for more minor components of the myelin sheath, such as myelin oligodendrocytic protein (MOG) are also important in some EAE models. Studies of MOG-induced EAE have shown that B cells and MOG-specific antibodies are important for initiation and pathogenesis of CNS autoimmune disease (11). T cell and antibody responses for myelin-associated oligodendrocytic basic protein (12-14) and other CNS antigens such as myelin-associated glycoprotein, CNPase, OSP, GalC, S100β and αβcrystallin have been studied but are not as well characterized as those for MBP, PLP and MOG (15). As in animal models, T cells specific for MBP, PLP and MOG have been detected in the peripheral blood of both MS patients and in healthy individuals (16). Presumably, these T cells in humans also have potential to mediate CNS autoimmune disease once they are activated, as observed in EAE.

Myelin Basic Protein

Immune tolerance mechanisms have been studied more for MBP than for any other CNS antigen. It is the primary target in many animal models of MS and its complex and developmentally regulated expression both within and outside of the

nervous system necessitates the usage of multiple mechanisms to maintain tolerance (17). The murine MBP gene locus contains eleven exons that encode two families of proteins, classic- and golli-MBPs, that are transcribed from three promoters within the locus (18, 19). Transcripts from both families undergo alternative splicing and produce multiple protein isoforms. The classic-MBP isoforms are major protein components of the myelin sheath in both the central and peripheral nervous systems comprising 30-40% and 5-15% of the total myelin protein, respectively (20). Classic-MBP is expressed primarily in myelin forming cells, oligodendrocytes and Schwann cells, where its primary function is to maintain the structure of the myelin sheath by contributing to the formation of the major dense line (21-23). Classic-MBP isoforms range in molecular weight from 14 kDa to 21.4 kDa. They are transcribed from the second and third promoter in the MBP locus, although only one described transcript is generated from the second promoter (M41) and this mRNA produces a protein identical to the 14 kDa classic-MBP isoform transcribed from the third promoter (24). Classic-MBP expression is developmentally regulated. In the mouse brain, classic-MBP expression begins between days 5 and 10 after birth. Active myelin formation occurs between day 10 and day 30 after birth, peaking at about day 18 (25, 26). The 14 kDa MBP isoform is the most abundantly expressed classic-MBP isoform in the nervous system. The next most abundant is the 18.5 kDa isoform followed by lower levels of the 17.2 kDa and 21.5 kDa isoforms (26). There is some research indicating that classic-MBP 14 and 18.5 kDa isoforms are expressed at low levels in lymph node macrophages (27) but expression of these isoforms is barely detectable.

The golli-MBP family of proteins are expressed from the most upstream promoter of the MBP locus. All golli-MBP transcripts contain the first three exons of the MBP locus (encoding 133 amino acids), which are unique to golli-MBP proteins. Alternative splicing of the remaining exons in the locus (exons 4-11) is used to generate the different golli-MBP isoforms. Three main transcripts have been described from the golli-MBP family. Two of these, BG21 and J37, generate proteins that have golli-MBP-specific N-termini but also share stretches of amino acid sequences with classic-MBP proteins. The

other major transcript, TP8, has a frame shift such that it does not contain any classic-MBP amino acid sequences (18). In addition to the three transcripts described above, Zelenika et al. isolated a novel golli-MBP transcript from a murine bone marrow cDNA library that contains all but exon 9 of classic-MBP (28).

Golli-MBP developmental expression, tissue distribution and function is different from classic-MBP. In the CNS, golli-MBP is expressed at high levels during embryonic development but then declines with age (18, 25, 28, 29). Golli-MBP proteins are detected in subsets of neurons in the CNS, (19, 30) and in nerve fibers in the CNS and peripheral nervous system (31, 32). Expression is not limited to the nervous system as golli-MBP is also found in primary and secondary lymphoid tissues. In the thymus, golli-MBP protein has been found mainly in thymocytes but can also be found in macrophages (33). The function(s) of the golli-proteins are not known, however, recent evidence suggests that they may play a role in neuronal process extension and myelination as well as being involved in the second messenger pathways that include PKC and MAP kinase in T cells (34).

T Cell Tolerance

In order to understand the pathogenesis of MS it is necessary to define the tolerance mechanisms that shape the auto-reactive T cell repertoire and regulate self-reactive lymphocyte responses. T cells will not be tolerized to a given antigen unless the antigen is processed and presented on MHC molecules in sufficient quantities to be recognized by the T cell. MHC class I-restricted $CD8^+$ T cells typically recognize protein epitopes synthesized within the cell while MHC class II-restricted $CD4^+$ T cells recognize epitopes derived from endocytosed proteins. The amount of a particular peptide/MHC complex on the cell surface of an antigen presenting cell (APC) depends on the amount of the protein available to the APC for processing, the efficiency of processing the particular epitope, the affinity of the peptide for the MHC molecule and the activation state of the APC (35). In the thymus, central tolerance is mediated predominantly by APCs in the medulla. If a thymocyte has a high avidity interaction with peptide/MHC on

an APC, the thymocyte is either deleted, becomes anergic or rearranges a different Vα gene segment to eliminate the self-reactive specificity (36, 37).

T cells that escape central tolerance are believed to be those that do not interact with self-peptide/MHC ligands in the thymus with sufficient avidity to undergo negative selection. Low avidity interactions between thymocytes and peptide/MHC ligands on APCs may be due to either 1) low affinity of a T cell receptor (TCR) for self-peptide/MHC complex (38, 39), or 2) self-peptide which does not bind well to the MHC (40). Once in the periphery, low avidity T cells are believed to ignore their self-antigen unless the self-antigen (or a mimic of the self-antigen) is presented in an immuno-stimulatory context. Once activated, these T cells should then be able to respond to lower levels of antigen with less dependency on co-stimulatory molecules. T cells would then be able to recognize the self-antigen in tissues where it was previously ignored. There is experimental evidence from several animal models of autoimmunity, including EAE, to support this idea (40-42).

While the above scenario could represent the initial steps in pathogenesis of autoimmunity in many cases, it is not clear that only T cells with low avidity for their self-ligands mediate autoimmune disease. It is possible that decreased efficiency of central tolerance in some individuals allows higher avidity T cells to escape from the thymus (43). Also, developmentally regulated proteins will not be constitutively present in the thymus, allowing some high avidity T cells for that particular antigen to escape during a specific time frame (44). Finally, high avidity T cells could escape central tolerance because they may not, by chance, encounter a thymic APC presenting their ligand. However, auto-reactive T cells with sufficient avidity to respond to their self-antigen in the periphery normally undergo peripheral tolerance if they encounter their peptide/MHC complex under non-immunostimulatory conditions. Passive peripheral tolerance mechanisms include deletion, induction of anergy, and TCR and/or co-receptor down-regulation (45, 46). Additionally, regulatory T cells can actively suppress self-reactive T cells that respond to self-antigens under non-inflammatory conditions in the periphery (47). The particular mechanism of peripheral tolerance acting on a self-

reactive T cell is believed to depend on the avidity of the interaction between the self-reactive T cell and the APC as well as the conditions under which the T cell encounters its antigen (48). Self-reactive lymphocytes circulate in the periphery of healthy individuals, therefore, decreased efficiency of any peripheral tolerance mechanism may pre-dispose an individual to autoimmunity.

Tolerance to CNS Antigens

Immune tolerance must be maintained to self-antigens expressed in tissues surveyed by the immune system. Tolerance to CNS antigens was previously thought to be less important because it was thought that CNS proteins were sequestered behind the blood brain barrier where there is limited access to cells of the immune system (49-51). However, more recent work has shown that lymphocytes, including naïve lymphocytes, may traffic through the CNS to a greater extent than was initially believed, implying that T cells specific for CNS antigens also need to undergo tolerance (52, 53). Recently it was shown that many "tissue-restricted" transcripts, including those encoding CNS proteins, are present in thymic APCs. A specialized set of medullary thymic epithelial cells (mTECs) appears to be the most promiscuous at expressing tissue-specific antigens (54). Along with many other tissue-restricted transcripts, DM20, a splice variant of the CNS myelin protein, PLP, is expressed in thymus (54-56). This expression is sufficient to induce central tolerance in the majority of PLP-specific T cells (56). These studies suggest that central tolerance plays an important role in eliminating CNS protein-specific T cells.

$CD4^+$ T Cell Tolerance to MBP in B10.PL Mice

As stated previously, EAE is induced by activating self-reactive T cells via immunization with myelin antigens in complete Freund's adjuvant or by adoptive transfer of activated myelin-specific T cells (8). In the susceptible B10.PL strain, almost all T cells primed by immunization with myelin basic protein (MBP) recognize a single MHC class II ($I\text{-}A^u$)-restricted epitope contained within MBPAc1-11 (57). Initially, this

observation was interpreted to mean that MBPAc1-11 was the only epitope processed from whole MBP that could be presented by I-A^u molecules and recognized by T cells. Previous studies in the Goverman lab showed that this is not the case by demonstrating that the MBP-specific repertoire in B10.PL mice is significantly influenced by immune tolerance mechanisms. Using the naturally occurring *shiverer* mutation which lacks exons 7-10 of the MBP locus and therefore does not make any classic-MBP isoforms ($MBP^{-/-}$ mice) (58-60), Harrington et al. demonstrated that immunization with whole MBP elicits strong T cell responses directed toward peptides within MBP121-150 while T cell responses to MBPAc1-11 are a minor component of the total MBP-specific response (61). In $MBP^{+/+}$ mice, MBP121-150-specific T cell responses in mice are mostly eliminated by tolerance mechanisms while MBPAc1-11-specific T cells escape tolerance.

It was proposed that the differential tolerance induction of MBPAc1-11 and MBP121-150-specific T cells was based on the relative affinities of the MBP peptides processed from these regions to I-A^u. Two synthetic peptides, MBP125-135 and MBP136-146, stimulate MBP-primed T cells from $MBP^{-/-}$ mice *in vitro* and both of these peptides exhibit high affinity for I-A^u (62). In contrast, MBPAc1-11 exhibits weak binding to I-A^u (63). These data suggested that one or both of the MBP125-135 and MBP136-146 epitopes are presented on the cell surface in greater abundance than MBPAc1-11 and therefore are more effective in mediating tolerance.

Analyses of TCR transgenic (Tg) mice supported this notion. MBP121-150-specific Tg T cells undergo central tolerance mediated by bone marrow-derived cells. The MBP121-150 epitopes are also presented constitutively in the periphery by APCs in sufficient quantity to activate naïve MBP121-150-specific Tg T cells isolated from $MBP^{-/-}$ mice and adoptively transferred into wild-type mice (44). However, studies of MBPAc1-11-specific TCR Tg mice indicated that insufficient ligand is presented by APCs *in vivo* to mediate central or peripheral tolerance induction of MBPAc1-11-specific Tg T cells (42, 64) or trigger their activation in the periphery following adoptive transfer (44).

The remainder of this thesis focuses on studies aimed at understanding processing and presentation of myelin basic protein in B10.PL mice and its impacts on T cell activation and tolerance. Chapter 2 describes the experimental methods. Chapter 3 shows data obtained in experiments designed to determine how a single MBP-specific TCR can recognize two dissimilar MBP peptides bound to the same MHC molecule. In Chapter 4, we define the MBP peptides that are processed and presented from intact MBP by antigen presenting cells to provide support for our model of differential epitope display affecting T cell tolerance induction to MBP. We describe the naturally processed peptides containing the MBPAc1-11 epitope and show that a binding register representing this epitope must compete with another more stable binding register within the processed peptide for binding to I-A^u. We also define the type of antigen presenting cells that present MBP epitopes to naïve Tg T cells *in vivo*, cells that presumably play a large role in peripheral tolerance of MBP-specific T cells. Chapter 5 shows experiments designed to understand why two different TCR Tg mouse lines specific for MBPAc1-11 exhibit different susceptibilities to spontaneous EAE.

Chapter 2: Materials and Methods

Mice

B10.PL mice (B10.PL-*H2*^{u} *H2-T18*^{a}/(73 NS)Sn) purchased from Jackson Laboratories (Bar Harbor, ME) were bred in a specific pathogen free facility at the University of Washington (Seattle). MBP$^{-/-}$ B10.PL mice, MBPAc1-11- and MBP121-150-specific TCR transgenic mice have been described previously (42, 44, 64). Thy1.1 mice (B6.PL-*Thy1*^{a}/Cy.J) were obtained from Jackson Laboratories (Bar Harbor, ME) and were backcrossed 8-10 generations onto the B10.PL background. Mice were bred and maintained in a specific pathogen-free (SPF) facility and all procedures involving animals were approved by the Animal Care Committee at the University of Washington.

Generation of Mutant MBP121-150-specific TCR Expression Vectors and Hybridomas

CDNAs encoding the α (Vα2.3) and β (Vβ8.2) chains of the 1.B2.D9 T cell hybridoma (61, 62) that is specific for MBP121-150 and cross-reactive to the two epitopes contained in MBP121-140 and MBP131-150 were each cloned into the pMI retroviral vector (65) under the LTR promoter. Single amino acid changes within the TCR α and β chains were introduced using the Quick-Change Site Directed Mutagenesis kit (Stratagene). For each mutagenesis, a restriction enzyme site was either deleted or added using synonymous amino acid changes near the desired mutation. Mutated plasmids were then transfected into Epicurian Coli® XL1-Blue supercompetent cells (Stratagene) and bacteria were screened using restriction enzyme digest of minipreps from single cell colonies. All mutated amino acids were changed to alanine except in the case of polar amino acids, which were changed to serine.

Retrovirus Production, Generation and Testing of Mutant MBP121-150-specific T Cell Hybridomas

Mutated and wild-type TCR α and β chain-encoding plasmids were transfected into the ϕNX-Ampho retroviral packaging cell line (P. Achacoso and G. Nolan, unpublished) using $CaPO_4$ precipitation as previously described (66). After overnight incubation at 32°C, retrovirus-containing supernatant was collected and used to infect a TCR^- DO11.10 hybridoma (67) or frozen at -80°C for use at a later time. TCR^- DO11.10 cells were infected by resuspending $5x10^5$ cells growing in log-phase in 1 mL retrovirus-containing supernatant supplemented with 5μg/mL polybrene. Cell suspension was spun for 90 minutes at 2500 rpm at room temperature, 1.5 mL fresh media was added and cells were incubated overnight at 32 °C. Two stably transduced DO11.10 clones expressing either the parent Vβ8.2 TCR chain or the Vα2.3 TCR chain were generated. These clones were then transduced with retrovirus encoding parent- or mutant- Vα2.3 chains or parent- or mutant- Vβ8.2 chains, respectively. After retroviral infection, cells were expanded for ~ 1 week. $V\alpha2.3^+$, $V\beta8.2^+$ and $CD4^+$ cells of the transduced cultures were sorted into a tube to generate a bulk culture and single cells were sorted into a 96-well plate (~1 cell/ well) to generate subclones. Bulk cultures of each hybridoma and expanded subclones with comparable levels of Vα2.3, Vβ8.2 and CD4 were tested for IL-2 production after stimulation with 1.9 and 0.95 μg/mL whole MBP, 6 and 2 nM MBP121-140 and 50 μM MBP131-150 as described previously (61). All antibodies used for experiments were purchased from BD Biosciences unless otherwise indicated.

Constructs, Expression and Purification of a Single Chain TCR

A soluble single chain TCR (scTCR) construct was made by linking DNA encoding the variable domains of the cross-reactive MBP121-150-specific 1.B2.D9 hybridoma by a 15 amino acid flexible linker (68) (Vβ8.2 amino acids 20-132 and Vα2.3 amino acids 30-139 joined by GSADDAKKDAAKKDG). The scTCR construct was placed in the NdeI and BamHI restriction sites of the pET22b expression vector under control of the T7 IPTG-inducible promoter. Plasmid was transfected into BL21 codon plus *E. coli* and protein was expressed as inclusion bodies. Inclusion bodies were

harvested and solubilized in 8 M urea, 100 mM Tris-HCL pH 8.0, 0.5 mM EDTA, 4 mM reduced glutathione, 0.4 mM oxidized glutathione, 0.5 mM PMSF and 50 mM glycine. Solubilized protein was refolded by dialysis at 0.5-1 mg/mL into 50 mM Tris pH 8.0, 2 mM EDTA, 400 mM L-arginine and urea, which was decreased in concentration 2-fold every 24 hours. When refolding solution was 0.5 M urea, protein was dialyzed into PNEA (150 mM NaCl, 1 mM EDTA, 0.02% NaN_3, and 25 mM PIPES pH 7.4), clarified by centrifugation and concentrated to ~2-4 mg/mL before purification via size exclusion chromatography on a Pharmacia/LKB Superdex 75 10/30 column in the Pharmacia/LKB FPLC system. Yield of refolded, concentrated (4-5 mg/mL) protein ranged from 0.5% to 2% of the initial protein concentration of solubilized inclusion bodies depending on the preparation. Refolded protein was run on a denaturing and non-denaturing PAGE to check for disulfide bond formation.

Sample Preparation for Mass Spectrometry

MBP was isolated using a protocol similar to that of Martenson et al. (69). Frozen whole mouse brains (Pel-Freez Biologicals) were minced and then ground to powder. Powder was homogenized in eight volumes of chloroform/methanol (2:1) and allowed to stand for 90 minutes at room temperature. Residue was washed in acetone (final solution = 90% acetone) for 30 minutes with stirring and centrifuged 15 minutes in a JA-17 rotor at 4°C. Pellets were dried overnight, homogenized in 1.4 volumes of 0.3 N HCl and incubated with stirring for 15 minutes at room temperature. The supernatant was further cleared by centrifugation at 5,000 RPM in a JA-17 rotor for 15 minutes (4°C) followed by ultracentrifugation at 25,000 RPM in an SW-28 rotor for 30 minutes (4°C). Supernatants were dialyzed against 10 mM acetic acid and lyophilized. Dried protein was resuspended in sterile 1X PBS. Splenocytes were prepared from $MBP^{+/+}$ and $MBP^{-/-}$ mice as described previously (70) and depleted of T cells using anti-TCR biotin (PharMingen) and streptavidin-labeled magnetic beads (Dynal). T-depleted splenocytes ($2x10^6$ cells/mL in RPMI) from $MBP^{+/+}$ and $MBP^{-/-}$ mice were incubated for 16 hours at 37° C with or without MBP (95 μg/mL), respectively. Two MBP-pulsed samples were

generated for this study, however only one of them was used to generate the final data set. One unpulsed sample from $MBP^{-/-}$ APCs was generated. Two unpulsed samples were also generated using $MBP^{+/+}$ T-depleted splenocytes, however, these were not used in the final subtractive analysis. $I\text{-}A^u$ was isolated and peptides eluted according to Luckey et al. (71) using the anti-$I\text{-}A^u$ 10-3.6.2 antibody (~ 1 mg/10^8 cells) bound to Protein A beads. Peptide was eluted with 10% acetic acid through a 10 kDa cutoff spinfilter (Millipore).

Mass Spectrometry

Approximately 6 x 10^6 cell equivalents (ce) of sample spiked with 2 fmol angiotensin I was gradient-eluted (C18 microcapillary, acetonitrile:water with 0.1 M acetic acid, 0-70% in 40 min at 57 nL/min) directly into a home-built Fourier Transform ion cyclotron resonance mass spectrometer (FT-ICR MS) as previously described (72). Full-scan mass spectra ($300 \leq m/z \leq 5{,}000$) were collected at approximately one scan per second, with typical resolution of 5,000-10,000 amu. Differential analysis of the FT-ICR MS to identify mass differences between data sets used a program designed by Dr. Dina Bai. The program aligned corresponding *m/z* values between data sets based on their elution points. Then multiple charged ions were deconvoluted to their +1 charge state and compared among data sets.

A list of masses present in one of the MBP-pulsed sample but not in the unpulsed sample ($MBP^{-/-}$ APCs) was generated. There were 673 masses in this data set and 100 differences were detected between two runs of the unpulsed ($MBP^{-/-}$ APCs) sample. Predicted masses for peptides containing MBP epitopes, MBPAc1-11, MBP125-135 and MBP136-146 were calculated (every combination of possible peptide masses was generated for up to 10 amino acids on either side of the core epitope) and compared to the list of masses obtained from the differential analysis. To verify MBP peptide identity assignments, about 6 x 10^7 ce of the MBP-pulsed sample were gradient eluted directly into a ThermoFinnigan LCQ Deca ion trap mass spectrometer (ThermoFinnigan) to collect ions with m/z of 300-2,000 amu. Predetermined precursor ions were then

subjected to collision-activated dissociation (CAD). The MS/MS spectra for each MBP candidate peptide in the sample were manually interpreted and compared to the MS/MS fragmentation patterns of synthetic peptides made based on known MBP peptide sequences. Co-elution studies were performed by adding 60 fmol of synthetic peptide to a 6 x 10^7 ce sample. Once MBP peptides were identified via comparison of the MBP pulsed and unpulsed sample derived from $MBP^{-/-}$ APCs, we searched for MBP peptides in the unpulsed sample from $MBP^{+/+}$ APCs and could not find any of the MBP peptides in this sample indicating that endogenously derived MBP peptides were not abundant enough to be detected by this methodology. Peptide concentrations/cell were estimated by normalizing the intensity of MBPAc1-18 peptide to the known amount of angiotensin I loaded with the sample. Concentrations of the other MBP samples were based on the concentration of MBPAc1-18. This was done because correction values for ionization efficiency differences between angiotensin I and the other MBP peptides were insignificant and therefore were not considered in the calculations.

Peptide Binding Assays

Peptides were synthesized using standard F-moc chemistry on an 433A peptide synthesizer (Applied Biosystems) and labeled with the *N*-hydroxysuccinimidyl ester of 5(6)-carboxyfluorescein before cleavage. Labeling was on either the N-terminus or, for N-acetylated peptides, on a C-terminal lysine selectively deprotected with 2% hydrazine. Peptides were cleaved from the resin (85% trifluoroacetic acid, 10% water and 5% thioanisole), purified by reverse-phase HPLC (C18, acetonitrile/water with 0.1% trifluoroacetic acid) and their identity confirmed by mass spectrometry. Detergent soluble $I\text{-}A^u$ was prepared as described previously (62). Briefly, cells expressing $I\text{-}A^u$ were lysed and $I\text{-}A^u$ isolated on a 10.3.6.2 affinity column. Protein was eluted with 0.2 M carbonate in 3 mM dodecyl maltoside at pH 11.5 and purity was assessed by silver-stained SDS-PAGE. A solution of $I\text{-}A^u$ (50-100 nM in 0.2 mM dodecyl maltoside/PBS) was incubated with excess peptide at pH 5.3 at 37 °C. Free, excess peptide was removed by size exclusion (Sephadex G50-SF) at 4 °C, pH 7.4 and the amount of peptide bound to

$I\text{-}A^u$ was assessed by high performance size exclusion chromatography (300 mm x 7.8 mm, Biosep-SEC-S 3000, Phenomenex) as the amount of fluorescence associated with the protein peak. Loss in fluorescence as a function of time was fit to an exponential function to obtain dissociation half-times.

Generation of MBPAc5-18-specific T Cell Hybridomas

MBPAc5-18 specific hybridomas were generated as previously described (61) using primed T cells from $MBP^{-/-}$ mice immunized with 156 μg MBPAc5-18 emulsified in CFA containing 0.5 mg/ml *Mycobacterium smegmatis*. IL-2 production by hybridomas was measured as described previously (61).

Stimulation of Naïve MBP121-150-specific Tg T Cells by APC Subsets

Naïve T cells from $MBP^{-/-}$ MBP121-150 TCR Tg mice and B cells were purified from spleen using AutoMACS (Miltenyi Biotec) magnetic cell separation. T cells were labeled with biotinylated anti-Vα2.3 and splenic B cells were labeled with biotinylated anti-B220. Both subsets were then incubated with streptavidin-conjugated microbeads (Miltenyi Biotec). For $CD11c^+$ (dendritic, DC) and $F4/80^+$/ $CD11c^-$ (macrophage) cell isolation, splenocytes were first depleted of TCR^+ and $B220^+$ cells using the AutoMACS. Depleted splenocytes were then stained with anti-F4/80-PE (Caltag) and anti-CD11c-FITC and sorted on a FACSVANTAGE cell sorter (BD Biosciences) into $CD11c^+$ cells and $F4/80^+/CD11c^-$ cells. Purity of populations assessed by flow cytometry was greater than 95% MBP121-150-specific Tg T cells, 95% for B cells, 92% for macrophage and 86% for $MBP^{+/+}$ DCs (10% of contaminants did not stain with anti-CD11c or F4/80) and 95% for $MBP^{-/-}$ DCs. APC subsets ($1x10^6$ bulk lymph node cells or splenocytes , $5x10^5$ B cells, $5x10^4$ dendritic cells or $8x10^4$ macrophages in each well) were cultured with $5x10^4$ MBP121-150-specific $V\alpha2^+$-purified T cells in 96 well round bottom plates in complete RPMI. Cultures were incubated 48 hours, pulsed with $[^3H]$-thymidine, and harvested 18 hours later. Stimulation index is calculated as the mean CPM of T cells

incubated with wild-type APCs divided by the mean CPM of T cells incubated with $MBP^{-/-}$ APCs.

Stimulation of Naïve MBP121-150-specific Tg T Cells by DC Subsets

MBP121-150-Tg T cells were isolated as described above. Three different methods were used to determine if $CD8\alpha^+$ or $CD8\alpha^-$ DCs (or both) present antigen to MBP121-150-specific T cells. 1) Spleen DC subsets were purified from splenocytes (non-collagenase-digested) using directly conjugated anti-CD11c microbeads (Miltenyi Biotec) and AutoMACS separation. Cells were then stained with anti-CD11c-FITC and anti-CD8α-Cychrome and sorted into $CD8\alpha^+$ and $CD8\alpha^-$ $CD11c^+$ subsets. Purity of subsets was >95%. Proliferation assays were set up as described above. In these experiments, however, cell viability, yield from the sorter and Tg T cell stimulation were low. 2) Lymph node DCs are better stimulators of naïve MBP121-150-specific Tg T cells but DCs are less abundant in lymph node versus spleen. To increase DC yield we purified DCs from collagenase-digested lymph node cells. Briefly, teased lymph nodes were subjected to mild collagenase digestion (Liberase RI, Roche, final enzyme concentration ~0.6 WU/mL) in the presence of 50 μg/mL DNase I (grade II, Roche) until tissues appeared fully digested (stirring ~45 minutes at 37 °C.). Digestion was stopped with addition of EDTA (10 mM final concentration), red blood cells were lysed and the sample was filtered through 70 μM nylon mesh. After collagenase digestion, samples were kept on ice in RPMI supplemented with 10% FCS, 20mM Hepes and 10mM EDTA (this media was used for all steps except the AutoMACs cell separation). For DC enrichment, T cells and B cells were removed via AutoMACS using anti-TCR and anti-CD19 biotinylated antibodies and streptavidin conjugated microbeads (Miltenyi Biotec). Enriched DCs were then stained with anti-CD11c-FITC and anti-CD8α-Cychrome and sorted into $CD8\alpha^+$ and $CD8\alpha^-$ DC subsets on an InFlux Flow Cytometer (Cytopeia). DCs were plated at $2x10^4$/well with $6x10^4$ T cells/well. Purity was above 79% in all samples but contaminating cells were mostly small $CD11c^-$ cells. 3) Total DCs or DC subsets were depleted from collagenase-digested lymph node cells stained with anti-

CD11c and anti-CD8. All DCs or either subset were depleted using a FACSVANTAGE cell sorter. Purity was not assessed for these samples as we would have had to collect our entire sample to determine the percentage of $CD11c^+$ cells removed from the sample. $1x10^6$ DC-depleted or non-depleted cells were plated in the presence of $5x10^4$ purified MBP121-150-specific Tg T cells/well.

Stimulation of Activated MBP121-150-specific Tg T Cells by APC Subsets

Activated T cells were prepared from spleen and lymph node cells harvested from $MBP^{-/-}$ MBP121-150-specific TCR Tg mice. Cultures were activated *in vitro* with 5 nM MBP121-150 in Click's media supplemented with 5% FBS, penicillin-streptomycin, 4 mM L-glutamine, 1 mM sodium pyruvate and 0.5 mM β-mercaptoethanol in a T-25 tissue culture flask at $3\text{-}5x10^6$ cells/mL. Four days after setup, cells were transferred to a T-75 flask and 10 mLs media with 10% FBS and 2.5 U/mL IL-2 was added. On day six, 10 more mLs 10% FBS/IL-2 media was added. On day seven, cells were centrifuged over a Lympholyte-M™ (Cedarlane Laboratories) gradient to remove dead cells, counted and put in complete RPMI prior to assay setup. B cells and dendritic cells were purified from collagenase-digested spleen or lymph nodes from both $MBP^{+/+}$ and $MBP^{-/-}$ mice. B cells were purified using anti-CD19-biotin followed by labeling with streptavidin-conjugated microbeads and AutoMACS. DCs were purified by labeling with CD11c-conjugated microbeads followed by AutoMACS separation. Cell subsets isolated from $MBP^{+/+}$ mice were greater than 96% pure and cells isolated from $MBP^{-/-}$ mice were greater than 92% pure as analyzed by flow cytometry. Naïve Tg T cells were isolated as described above. Naïve and activated T cells were plated at $8x10^4$/well along with $CD11c^+$ DCs, $CD19^+$ B cells and whole LN or SPL (at $8x10^4$, $7x10^5$ or $1x10^6$/ well, respectively).

Purification of MBPAc1-11-specific Tg1 and Tg2 T Cells for Proliferation Assays and APC Fixation

T cells from MBPAc1-11-specific TCR Tg mouse lines (Tg1 and Tg2) (42, 64) were isolated in the same way as MBP121-150 Tg T cells described above except that either anti-Vβ8.2-biotin or anti-CD4-biotin antibodies were used for positive purification and a $CD4^+$ T cell isolation kit (Miltenyi Biotec) was used for purification via negative selection. Equal numbers of $V\beta8.2^+CD4^+$ Tg T cells from each strain were plated at 8 $x10^4$-$1.5x10^5$ Tg T cells per well with $1x10^6$ irradiated syngeneic APCs and indicated concentration of whole MBP, MBPAc1-11 or MBPAc1-18. Proliferation was measured as described above. In experiments utilizing fixed APCs, splenocytes were washed two times with PBS and then resuspended in 0.1% cold paraformaldehyde at $3.3x10^6$ cells/mL and incubated at room temperature for 4 minutes. Cells were then washed three times in PBS. Antigen was added to APCs after fixation.

Generation of Activated MBPAc1-11-specific Tg1 and Tg2 T Cells

Tg1 and Tg2 T cells purified via negative selection were activated in the presence of irradiated $Thy1.1^+$ APCs and 3.2μM MBPAc1-11 or 10.5 μg/mL (Experiment 1) or 21 μg/mL MBP (Experiment 2) in 10 mL media. Cells were cultured as described for activated MBP121-150 Tg T cells.

Intracellular Cytokine Staining of MBPAc1-11-specific Tg1 and Tg2 T Cells

Assays were set up in 96 well round bottom plates with $1x10^5$ Tg1 or Tg2 T cells, $9x10^5$ $Thy1.1^+$ APCs, 10μM MBPAc1-11 or 21 (Experiment 1) or 105 (Experiment 2) μg/mL whole MBP. Cells were incubated for various time points as indicated in Figures 14 and 15. Golgi-stop/plug (BD Biosciences) was added for the last eight hours of the incubation. After the incubation, cells were washed with PBS and surface stained with anti-Thy1.2-FITC and anti-CD4-Cychrome (Experiment 1) or anti-Thy1.2-FITC and anti-CD4-PE Texas Red (Caltag) (Experiment 2). After surface staining, cells were washed with PBS and stained for intracellular cytokines immediately or up to 18 hrs later (stored at 4 °C in PBS without fixing). Intracellular cytokine staining was done according to the BD Cytofix/Cytoperm™ Kit Manual. Anti-cytokine antibodies (BD Biosciences) used in

Experiment 1 were PE-labeled anti-IFN-γ, anti-IL-2 and anti-TNF-α. In Experiment 2, PE-labeled anti-IFN-γ, anti-IL-2, anti-IL-4 and anti-TNF-α APC were used and cells were double stained for anti-TNF-α and anti-IL-4. Cells were analyzed on a FACScan LSR (BD Biosciences) flow cytometer within two days of staining.

Chapter 3: Structural Basis for TCR Cross-reactivity

Introduction

Studies investigating T-cell tolerance induction to MBP in B10.PL mice showed that T cells specific for MBP121-150 could be isolated from $MBP^{-/-}$ mice (61). MBP121-150-specific T cells differed in their responses to 20-mer peptides within MBP121-150. Interestingly, one group of MBP121-150-specific T cells was able to respond to two synthetic peptides, MBP121-140 and MBP131-150. Responses were elicited by two non-overlapping epitopes defined by the core epitopes, MBP125-135 and MBP136-146, which both bind stably to $I\text{-}A^{u}$. Amino acid substitutions of peptide residues elucidated the functional contacts for this cross-reactive TCR and these contacts were chemically very dissimilar for each epitope. Exchanging the primary TCR contact residues at the same position in both epitopes abolished cross-reactive T cell responses (62) indicating that the TCR was not seeing both peptides on the basis of chemical similarities of the TCR contacts. Instead, the cross-reactive MBP121-150-specific TCR recognizes MBP125-135 and MBP136-146 peptides in a "context-sensitive" fashion (62). We hypothesized that the MBP121-150-specific cross-reactive TCR uses different amino acids within the complementarity-determining regions (CDRs), hypervariable regions of the TCR that contact the peptide/MHC surface, to recognize the two different peptides.

Mutational Analysis of a Cross-reactive MBP121-150-specific TCR

To determine if plasticity in TCR recognition of MBP121-140 and MBP131-150 is due to differences in the TCR residues that interact with each ligand, we carried out mutational analyses on the TCR genes (Vα2.3 and Vβ8.2) cloned from a cross-reactive T cell hybridoma. Both CDR1 and CDR3 have been shown in structural studies to contact the peptide, whereas CDR2 of the TCRα and TCRβ chains mainly contact the MHC (73, 74). A panel of single amino acid mutations within the CDR1 and CDR3 loops of the TCR Vα2.3 and Vβ8.2 chains was generated using site-directed mutagenesis. Mutant TCRs were transduced into a TCR^{-} DO11.10 T cell hybridoma. IL-2 responses to the

different MBP epitopes were compared between the mutant TCR-transduced hybridomas and parent TCR-transduced hybridomas. Mutant TCR-transduced hybridomas that had levels of Vα2.3, Vβ8.2 and CD4 surface staining similar to the wild-type TCR-transduced hybridomas were selected for analysis (data not shown). Mutations that allow the TCR to respond to whole MBP and only one of the two peptides within MBP121-150 would indicate that this mutation is involved in recognition of one epitope but not the other.

Mutations either had no effect or affected responses to both MBP121-140 and MBP131-150. Figure 1 shows data from an IL-2 assay comparing two TCR mutants, one that abolishes MBP epitope recognition and one that behaves like the wild-type TCR. Of the mutants analyzed, 12/15 mutations made within the Vα2.3 and Vβ8.2 CDR3 regions abolished IL-2 responses to whole MBP and both MBP121-150 epitopes (Figure 2). One mutation, N100A, in the CDR3 region of the TCR β chain decreased responses to both epitopes, compared to wild-type TCR responses. From the CDR1 regions, only 4/13 mutants abolished MBP epitope recognition (Figure 2) and one mutation (M32Aα) was unable to produce surface TCR. No mutants were found in either CDR region that abolished responses for only one of the MBP epitopes. These data, although incomplete, suggest that the TCR uses the same residues (at least within CDR1 and 3) to recognize both epitopes within MBP121-150.

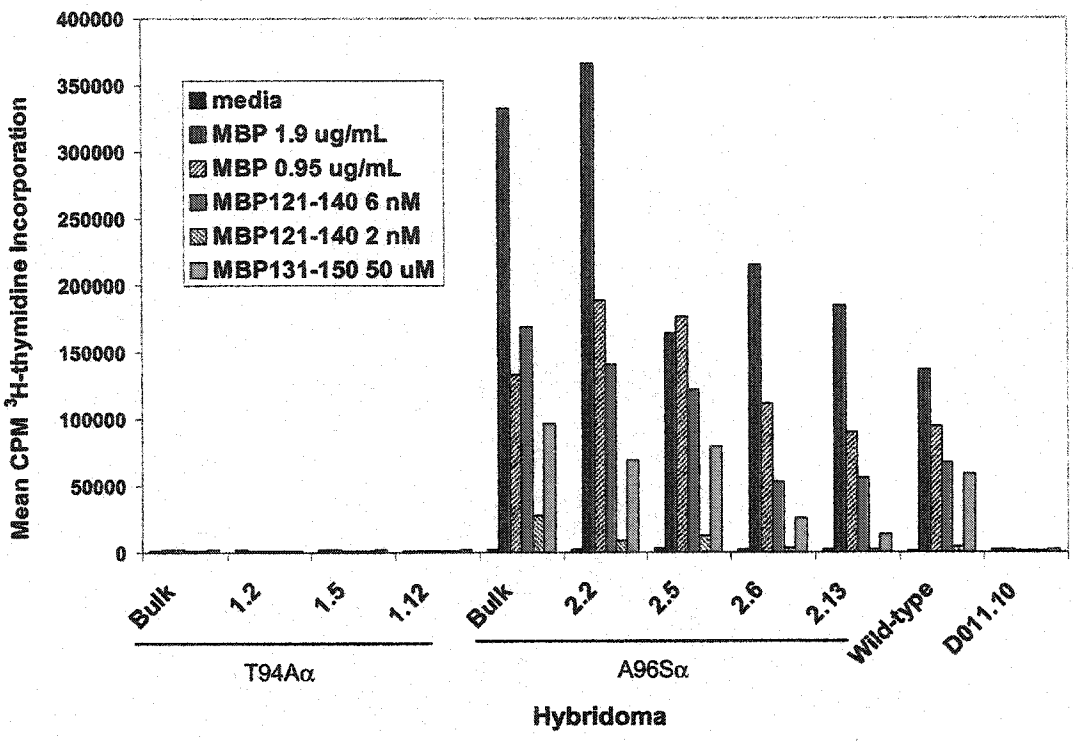

Figure 1. Mutations within the CDR regions of a cross-reactive MBP121-150-specific TCR had either no effect or affected recognition of both MBP121-150 epitopes. This is an example of the assay used to screen the mutant TCR-transduced hybridomas. Retrovirally transduced hybridomas were sorted based on Vα2.3 or Vβ8.2 expression into 96 well plates and expanded. A bulk liquid culture ($2x10^5$-$1x10^6$ cells/starting culture) was also sorted and expanded. Several $CD4^+V\alpha2.3^+V\beta8.2^+$ clones from each mutation (numbered clones), as well as the expanded bulk culture (bulk) of each mutation were tested for their ability to respond to the indicated concentrations of MBP, MBP121-140 and MBP131-150. These responses were compared to the responses of a wild-type clone (Wild-type) and the non-transduced hybridoma (DO11.10). Shown here are data for two mutations within the CDR3 region of the TCR α chain. The T94A mutation abolished responses to MBP epitopes, while the A96S mutation behaves like wild-type.

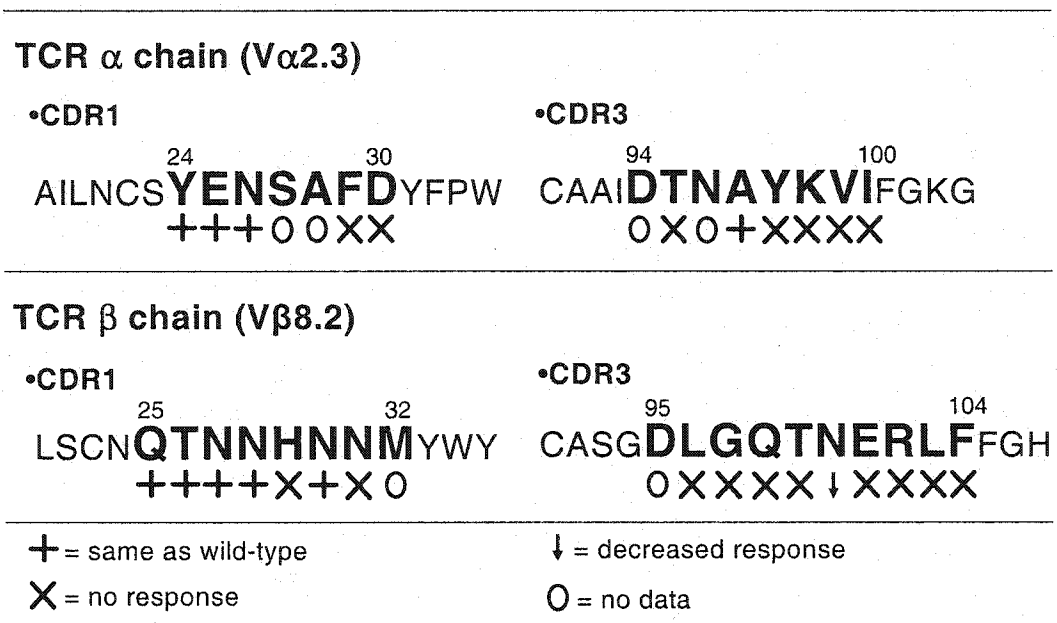

Figure 2. Summary of CDR mutation results for the MBP121-150 TCR. Sequences of the CDR1 and 3 regions (bolded, large font within sequence) of the TCRα (upper sequences) and TCRβ (lower sequences) are shown. Numbers indicate amino acid number of each chain for reference.

Recognition of MBP131-150 is Dependent on CD4

During initial attempts to express the wild-type MBP121-150-specific TCR in the DO11.10 hybridoma, we obtained clones that would only respond to MBP121-140 and not to MBP131-150. Further work demonstrated that some of our clones did not express CD4 and these would not respond to MBP131-150 while the $CD4^+$ clones were able to respond to both epitopes (SI to MBP121-140, MBP131-150, respectively: $CD4^+$=11, 9 $CD4^-$=7, 0.9). These data indicate that the response to MBP131-150 is dependent on CD4 expression while the response to MBP121-140 is not.

Crystal Structures of the MBP121-150-specific TCR Binding to the Two Ligands

The mutational analysis of the CDRs, although incomplete, indicated that it was unlikely that this approach would be able to define how a single TCR can cross react with two dissimilar peptides. Crystal structures of the trimolecular complex consisting of the

cross-reactive MBP121-150-specific TCR binding to MBP125-135/I-A^u and 135-146/I-A^u would elucidate the molecular details of how the same TCR binds to two different epitopes. Collaboration with Dr. Roland Strong's laboratory was initiated to determine if soluble TCR and MHC molecules could be expressed and purified. We were able to express the extracellular domain of this MBP121-150-specific TCR in *Escherichia coli* and were able to purify refolded TCR using size exclusion chromatography (results not shown). Wendy Paulsene in Dr. Strong's laboratory will investigate whether it will be possible to express the soluble portions of the I-A^u α and β chains in bacterial inclusion bodies so that it can be refolded in the presence of multiple peptides. If this can be done, it may be possible to generate a trimolecular crystal structure of the MBP121-150-specific TCR binding to MBP125-135/I-A^u and 135-146/I-A^u.

Discussion

Although each TCR interaction with peptide/MHC (pMHC) is unique with demonstrated flexibility in the TCR footprints on the pMHC for each TCR, analysis of TCR crystal structures indicates that there is a general mode of binding of the TCR to the pMHC (75). These studies show that the Vα domain is closer to the N-terminus of the bound peptide while the Vβ domain is closer to the C-terminus with a roughly diagonal docking mode. The TCR can bind across the pMHC but the diagonal can vary between 45-80° compared to the axis going through the length of the peptide bound to MHC (75). This docking mode tends to place the CDR3 loops of the TCR variable domains over the peptide bound to MHC. The CDR1 loops of both chains can interact with both the peptide and MHC while the CDR2 loops predominantly interact with MHC residues (73, 74). The CDR3 region also tends to be the most flexible part of the pMHC binding region (when overlays of the different structures are compared) and is the most variable in amino acid composition and length (74). This flexibility may influence the TCR's ability to accommodate multiple binding specificities and also suggests that the CDR3 loops will be important in specific TCR/peptide interactions, even though they also can contact MHC residues (76).

The flexible nature of TCR binding has been demonstrated experimentally by analyzing the responses of clonal T cells to multiple ligands. Earlier studies involved the use of altered peptide ligands (77) or peptides demonstrating molecular mimicry, where peptides of similar shape and charge can interact with a single TCR (78) to define the degree of changes tolerated by a single TCR for binding. More recently, studies identifying agonist peptide motifs for TCRs of unknown specificity using large synthetic peptide libraries also demonstrated extensive TCR cross-reactivity, even to unrelated peptides (79). Our studies involve the use of a TCR that recognizes two peptides derived from an autoantigen that bind the same MHC molecule with high affinity yet are structurally unrelated in the surfaces presented to the TCR (62). We wanted to understand how the same TCR can bind to such different surfaces.

We tested the hypothesis that the MBP121-150-specific TCR uses different amino acids within the CDRs to contact the amino acids of the peptides. This hypothesis predicts that some of the mutations made within CDR1 and CDR3 would affect T cell responses to only one of the two MBP121-150 epitopes. However, this mutational analysis failed to detect any single amino acid changes that affected binding to only one of the epitopes. Most of the mutations made in the CDR3 region abolished TCR responses to both epitopes, consistent with the concept that this loop is the primary region of the TCR involved in peptide recognition. Some of the mutations may have interrupted binding between the TCR and MHC. In several TCR/pMHC class I structures, the tips of the CDR1 and 2 loops are mostly involved in binding to the MHC molecule and these tips correspond to the same sequence positions from one TCR to another. Within CDR1α and β, amino acid residues 27-30 contact the MHC (74). Three mutations made in this region, F29A and D30A of CDR1α and H29A in CDR1β abolished recognition of all MBP epitopes and this could be due to lack of binding with the MHC molecule itself rather than the peptide.

Generation of a crystal structure of the MBP121-150-specific TCR bound to the two different MBP121-150 epitopes in I-A^u is a difficult task, but may be the only way to understand the basis for cross-reactivity of this TCR. It is possible that the TCR loops

adopt slightly different conformations or that the plane of the TCR binding surface is tilted to allow recognition of the different peptides. Both of these possibilities would be elucidated in a structure of the two complexes.

The TCR requires CD4 to interact with the MBP131-150 epitope but not for the MBP121-140 epitope even though binding to I-A^u between the two epitopes is similar (62) indicating that the interaction between the cross-reactive MBP121-150-specific TCR and MBP131-150 is lower affinity than for MBP121-140. This is also supported by the fact that over 8000 times more MBP131-150 (50 μM) than MBP121-140 is required to consistently detect T cell hybridoma responses to this peptide. Although the structural aspects of the MBP121-150 TCR cross-reactivity are interesting, the cross-reactivity of this TCR to MBP131-150 is most likely not relevant to tolerance induction because it does not appear to be processed from whole MBP (see Chapter 4).

Chapter 4: Processing and Presentation of MBP; Generation of N-terminal MBP Peptides with Competing MHC Binding Registers Affects MBP-specific T Cell Tolerance

Part A. MBP Processing

Introduction

The synthetic peptides used to define MBP121-150 (61, 62) and MBPAc1-11 (57) epitopes have large differences in affinity for I-A^u suggesting that, if processed equally, MBP121-150 peptides should be presented at higher abundance than MBPAc1-11 peptides on APCs *in vivo* because they form more stable complexes. This differential epitope display hypothesis would explain the differential tolerance induction seen between MBP121-150 and MBPAc1-11-specific Tg T cells.

The use of synthetic peptides to assess T cell responses *in vitro* is a concern for several reasons. Recent studies have shown that peptides that are not obtained from processing sometimes bind in a different conformation compared to those derived from processing of the intact protein (80, 81). It is unlikely that this is the case for MBP121-150 or MBPAc1-11-specific T cells as both T cells were generated from mice immunized with whole MBP and the T cells respond to both synthetic peptides and whole MBP. However, the peptides used in the epitope mapping of MBP-specific T cells may not reflect what is actually processed from whole protein under non-inflammatory, tolerizing conditions *in vivo*. Amino acids flanking a core epitope can influence binding to the MHC by interacting more or less favorably with MHC residues outside of the binding groove (82). It is also possible for processed peptides to contain multiple epitopes that compete for binding to the MHC (83). In order to address the caveats associated with the use of synthetic peptides, provide direct support for our model of differential epitope display, and to determine if both epitopes within MBP121-150 are processed from whole MBP, we analyzed peptides eluted from I-A^u molecules that were purified from whole MBP-pulsed splenocytes. Based on the affinity differences between MBPAc1-11 and

MBP121-150 epitopes, we expected to detect predominantly peptides derived from MBP121-150 and few or no peptides containing MBPAc1-11. We also looked specifically for peptides containing either MBP125-135 or MBP136-146.

MBP Processing Generates at Least Two Different Nested Sets of Peptides

Differential analysis was used to identify peptides that were processed from whole MBP by APCs and presented on I-A^u. Splenocytes from B10.PL mice were incubated overnight with whole MBP in order to enrich the amount of MBP peptides associated with I-A^u on the cell surface. This MBP-pulsed sample was compared to an unpulsed sample of splenocytes isolated from $MBP^{-/-}$ B10.PL mice incubated without MBP. I-A^u molecules were purified from both the MBP-pulsed and unpulsed samples and peptides were eluted. Peptide masses were analyzed using Fourier transform ion cyclotron resonance mass spectrometry (FT-ICR-MS). Total ion chromatograms for each sample are shown in Figure 3. Subtractive analysis software was used to identify peptides present in the MBP-pulsed FT-ICR-MS data set that were absent in the negative data set.

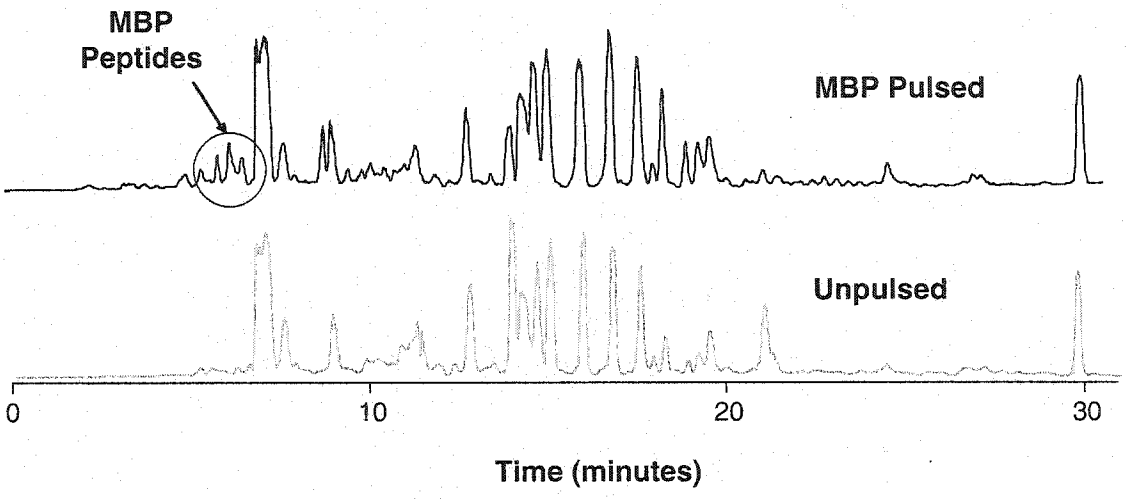

Figure 3. FT-ICR-MS total ion chromatograms (TIC) of peptides eluted from MBP-pulsed and unpulsed samples. All MBP peptides identified were eluted in the region circled in the MBP-pulsed TIC. Mass spectra were recorded at 1 s intervals and the majority of the peptides eluted within a ~28 min period of the gradient.

Peptides bound to MHC class II molecules are typically identified as nested sets, consisting of variable length peptides (between 12 and 18 amino acids) all containing a core peptide sequence that binds in the MHC binding groove. Variable peptide termini may arise from non-specific peptidase activity that trims peptide ends not protected by the MHC binding groove (35). Nested sets of peptides were identified from two regions within MBP (Table 1.). Collision-activated dissociation (CAD) analyses (Figure 4) and co-elution (Figure 5) were used to confirm the identity of multiple peptides from each nested set (Table 1). One peptide set corresponded to the N-terminus of MBP and the other set was derived from the MBP121-150 region. The most abundant MBP peptides eluted from I-A^u were MBPAc1-17 and MBPAc1-18. The nested set containing MBPAc1-17 and MBPAc1-18 was approximately 23 times more abundant than the peptide set derived from the MBP121-150 region. Within the MBP121-150 region, only peptides containing the predicted core epitope MBP125-135 were found. No peptides containing the MBP136-146 predicted epitope were identified at our detection limit (estimated to be one copy/cell).

Table 1. MBP peptides eluted from I-A^u identified by mass spectrometry

MBP Peptide[a]	Mass (Observed)	Mass (Calculated)	Scan #	Abundance	Copy/ cell[b]	CAD[c]
3-16	545.307	545.309	153	11.7	2.4	
3-17	430.994[d]	430.992	204	51.9	10.4	
2-16	430.994[d]	430.992	204	51.9	10.5	
4-17	531.634	531.634	190	181.6	36.3	YES[e]
Ac1-16	612.010	612.003	321	90.8	18.1	
Ac1-17	641.015	641.013	311	2410.9	484.0	YES[e]
Ac1-18	674.696	674.696	328	3112.8	622.0	YES[e]
Ac1-19	718.738	718.718	438	33.4	6.7	
Ac1-20	756.738	756.718	439	122.1	24.4	
Ac1-22	619.823[d]	619.814	428	28.4	5.7	
124-137	499.583	499.580	183	46.2	9.2	YES
124-138	548.609	548.602	319	32.5	6.3	YES
123-138	567.616	567.610	317	31.4	6.5	YES
123-136	499.583	499.580	183	46.2	9.2	YES
122-136	548.609	548.602	319	32.5	6.3	YES[e]
121-136	567.616	567.610	317	31.4	6.5	YES
122-137	567.616	567.610	317	31.4	6.5	
120-137	450.227[d]	450.222	363	16.8	3.4	

[a]Peptide identity was assigned by matching the observed and calculated masses. Numbering is based on the sequence of the 18.5 kDa MBP isoform.
[b]Based on copy number/cell of MBPAc1-18 which was determined by comparison to angiotensin control.
[c]Peptide identities assigned in column one were confirmed by CAD analysis.
[d]Observed masses are from +4 charge state peptides, all other masses are from +3 charge state peptides.
[e]Identities were also confirmed by co-elution experiments.

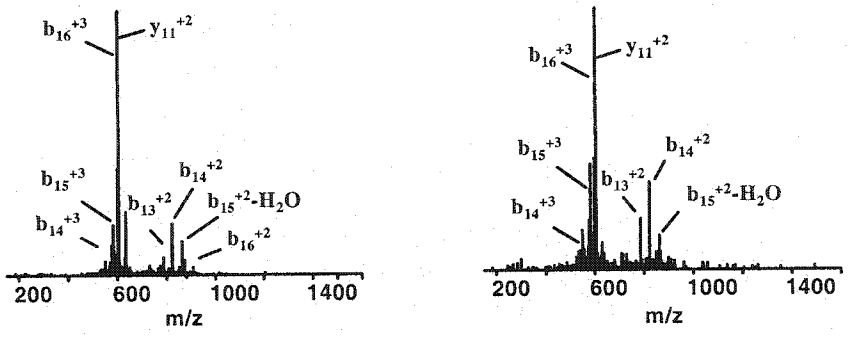

b_n^{+2}	57	101	165	229	307	355	399	463	541	585	649	730	787	822	873	909	961		
Ac-	A	S	Q	K	R	P	S	Q	R	S	K	Y	L	A	T	A	S		
	961	905	861	797	733	655	606	563	499	420	377	313	231	175	139	89	53	y_n^{+2}	

Figure 4. Confirmation of candidate masses identified in the subtractive analysis of the FT-ICR-MS data by partial peptide sequencing (example: Ac1-17). Synthetic peptide was loaded onto an ICR mass spectrometer and subjected to collision activated dissociation (CAD). This spectra was then compared to the spectra obtained from CAD of the candidate MBPAc1-17 peptide from the MBP-pulsed sample. The CAD spectra shown are for synthetic (left) and sample (right) MBPAc1-17. The sequence (bottom) shows the masses of ions that may be generated by CAD of MBPAc1-17. Underlined masses were found both in the spectra for synthetic and sample MBPAc1-17.

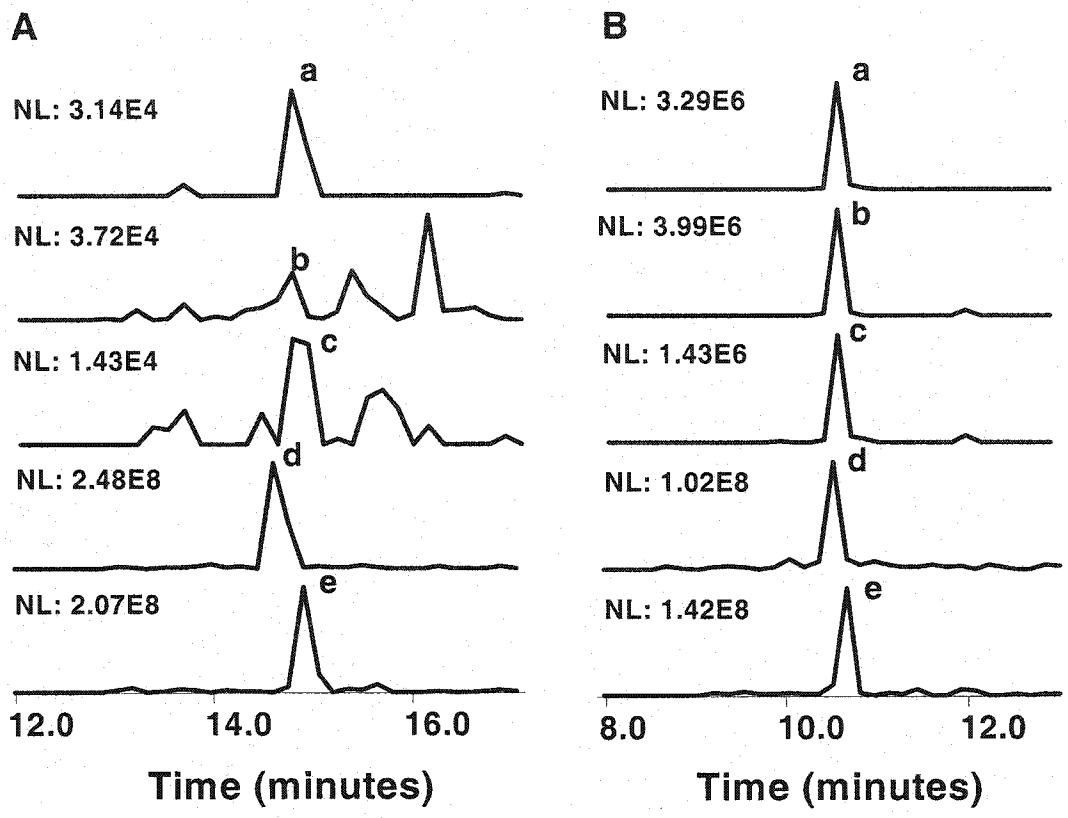

Figure 5. Confirmation of candidate masses identified in the subtractive analysis of the FT-ICR-MS data by co-elution (example MBP122-136). The selected ion chromatogram (SIC) for the MBP pulsed sample without synthetic peptide added (A) and the MBP pulsed sample with 60 fmoles of synthetic MBP122-136 peptide added (B) were compared. The SIC for fragment ions derived from MBP122-136 peptide (a-c) are detected at times between the detection of ions derived from MBPAc1-17 (d) and MBPAc1-18 (e). The co-elution shows the relative abundance of each fragment ion derived from MBP122-136 peptide in the MBP pulsed sample increased by a factor of 100 when co-eluted with 100 times more synthetic MBP122-136, while the MBPAc 1-17 and MBPAc 1-18-derived fragment ions remained the same.

The Stable MBP5-16 Binding Register Accounts for the Abundance of N-terminal Peptides

In contrast to our prediction that we would see predominantly MBP121-150 peptides eluted from MBP-pulsed APCs, peptides derived from the N-terminus are the most abundant peptides generated by processing MBP despite the low binding affinity of

the only known T cell epitope in that region, MBPAc1-11, for I-A^u. The higher than expected abundance of these peptides could be due to the presence of a second, more stable I-A^u binding register within the N- terminus, MBP5-16, that has been previously described (57, 84, 85). MBP5-16 binds I-A^u with high affinity by placing a favorable tyrosine residue (MBP12) in the p6 pocket of I-A^u (Figure 6) (84). Binding in the MBP5-16 register would be favored relative to the MBPAc1-11 register, which places an unfavorable lysine (MBP4) in the p6 pocket (63). Previous studies that described the MBP5-16 binding register concluded that processed peptides derived from whole MBP could not contain both MBPAc1-11 and MBP5-16 (57, 84, 85). This conclusion was based on observations that T cell hybridomas specific for MBPAc1-11 could not be stimulated by peptides containing both binding registers on fixed APCs (57, 84). Our data demonstrating that MBP processing primarily generates N-terminal peptides containing both registers required us to reconsider the interpretation of these results.

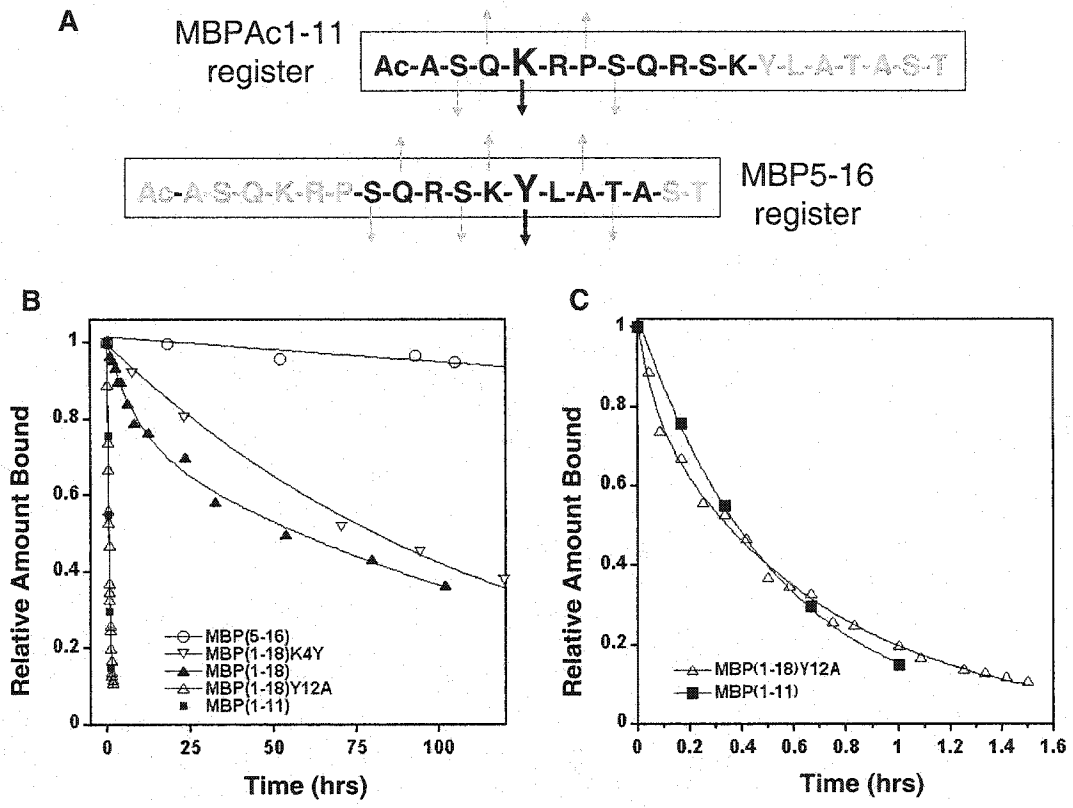

Figure 6. MBPAc1-18 contains two MHC binding registers and demonstrates biphasic dissociation from I-A^u. Two different binding registers of Ac1-18 are shown in bold type (A). The amino acid that binds in the p6 pocket for each register is in larger type, with a bold arrow pointing down. Other grey down-arrows indicate amino acids that point toward I-A^u while the grey up-arrows indicate amino acids that would be potential TCR contacts. Dissociation of fluorescein-labeled MBP peptides from soluble I-A^u (B and C) demonstrates biphasic dissociation of MBPAc1-18 (B) while analogue peptides mutated to disrupt binding of the peptide in the p6 pocket of I-A^u for each register dissociate with monophasic kinetics (B and C). For MBPAc1-18, ~38% of the original peptide bound was bound in the faster phase: $t_{1/2}$fast=3.7 h. About 62% of the initial peptide is bound in the slow phase: $t_{1/2}$slow=117 h. (C) Expanded time-scale of (B) showing the monophasic, fast dissociation of MBPAc1-18Y12A and MBPAc1-11. Peptide loading onto soluble I-A^u was done for one hour at 37 °C at pH 5.3.

We investigated whether the N-terminal peptides could bind I-A^u using both binding registers by analyzing the kinetics of dissociation of MBPAc1-18 and the shorter

peptides representing the individual binding registers of MBPAc1-18 from solubilized I-A^u. MBP5-16/I-A^u dissociated so slowly that a half-life was difficult to measure ($t_{1/2}$ > 1000 hrs; Figure 6B). The half-life of MBPAc1-11/I-A^u was only 30 minutes. Interestingly, MBPAc1-18/I-A^u dissociated with biphasic kinetics, indicating that the peptide binds in a mixture of short-lived and long-lived complexes (Figure 6B). Under the binding conditions used in this experiment (peptide incubated with MHC molecules for one hour at 37°C at pH 5.2), approximately 38% and 62% of the MBPAc1-18 peptides formed short- and long-lived complexes, respectively. Increasing the incubation time of the MBPAc1-18 peptide with soluble I-A^u from one to 16 hours increased the amount of peptide bound in the long phase to 77% (data not shown). To confirm that the slow-dissociating phase corresponded to peptides bound in the MBP5-16 register and the rapid-dissociating phase to peptides bound in the MBPAc1-11 binding register, dissociation of analogue peptides with mutations in the p6 anchor residues for each register was analyzed. The MBPAc1-18Y12A substitution, which abrogates binding in the MBP5-16 register, exhibits single phase, rapid dissociation that is essentially identical to the dissociation rate of MBPAc1-11 (Figure 6B and C). Conversely, the MBPAc1-18K4Y substitution, which replaces the unfavorable lysine in the anchor position of the MBPAc1-11 register with a highly favorable tyrosine residue, converts the MBPAc1-18 peptide into a single phase, slow-dissociating peptide whose half-life is very similar to the slow phase of native MBPAc1-18 (Figure 6B). These data confirm the utilization of the MBPAc1-11 and MBP5-16 binding registers within MBPAc1-18 and suggest that most, but not all, of MBPAc1-18 is bound to I-A^u in the MBP5-16 register.

MBPAc1-11-specific T Cells Recognize MBPAc1-18/I-A^u Complexes on Fixed APCs

The data described above suggest that priming of MBPAc1-11-specific T cells by immunization with whole MBP *in vivo* occurs through recognition of the relatively small amount of N-terminal peptides (predominantly MBPAc1-18 and Ac1-17) bound in the MBPAc1-11 register. This interpretation predicts that MBPAc1-11-specific T cells should be able to respond to MBPAc1-18 without additional processing. To test this

prediction, we analyzed T cell proliferation of T cells purified from two different MBPAc1-11-specific TCR Tg lines (42, 64) incubated with MBPAc1-18 and live or paraformaldehyde-fixed APCs. While only live APCs could present whole MBP to the T cells, both types of T cells responded well to MBPAc1-18 and MBPAc1-11 on fixed APCs (Figure 7).

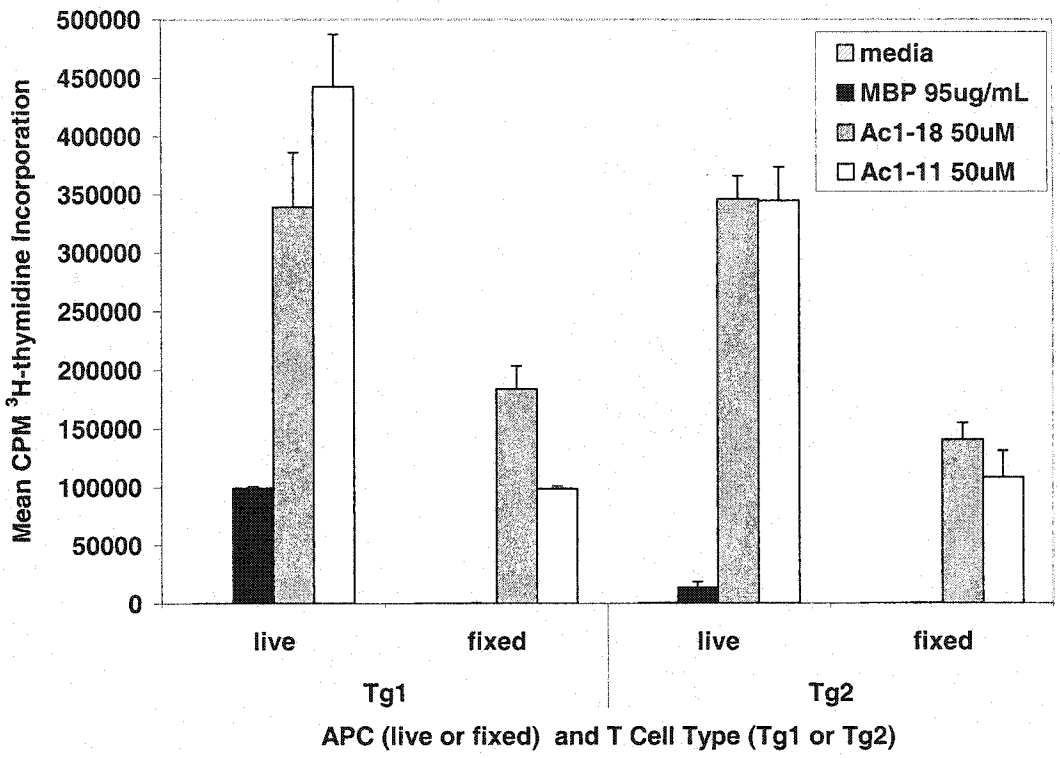

Figure 7. MBPAc1-18 is able to stimulate Ac1-11-specific T cells when presented by fixed APCs. Naïve MBPAc1-11-specific transgenic T cells were purified from two different Tg lines (Tg1 and Tg2) by autoMACs using either anti-Vα2.3 (Tg1) or Vβ8.2 (Tg2) biotinylated antibodies. T cells were further purified by sorting away I-A^u positive cells. $1x10^5$ T cells were plated in the presence of $1x10^6$ live or fixed APCs. Responses to whole MBP were measured as a control for fixing and to MBPAc1-11 as a positive control. T cells alone did not proliferate above background in the presence of peptide (data not shown). Tg2 responses to MBP on live APCs are much lower than Tg1 responses but the stimulation is still 28 times background. Error bars represent one standard deviation of triplicate wells.

MBP5-16-specific T Cells

Original studies describing an H-2^u-restricted T cell epitope in addition to MBPAc1-11 within the N-terminus of MBP were able to detect T cell responses to MBP9-20 after immunization of mice with whole rat MBP. However, unlike T cells specific for MBPAc1-11, MBP9-20-specific T cells were not encephalitogenic (57, 85). In later studies Fairchild et al. could not detect T cell responses to MBP5-20 or 9-20 in mice immunized with whole mouse MBP (84) and concluded that peptides containing the MBP5-16 register were either not naturally processed or that MBP5-16-specific T cells were tolerized in wild-type mice. The discrepancies in these results could be explained by sequence differences between rat and mouse MBP in the N-terminus. Another difference in these studies was that Fairchild et al. used PL/J (H-2^u) mice and both earlier studies used F_1 mice generated by crossing the PL/J and SJL (H-2^s) strains.

To further investigate T cell tolerance to MBP5-16, $MBP^{-/-}$ B10.PL mice were immunized with whole MBP and draining lymph node T cell responses to whole MBP, MBP121-140, MBPAc1-18, MBPAc1-11, and MBPAc5-18 were analyzed. T cell responses to MBPAc5-18 were undetectable even though responses to MBPAc1-11, MBPAc1-18 and MBP121-140 could be detected (data not shown). However, MBPAc5-18-specific T cell hybridomas could be generated by immunizing $MBP^{-/-}$ mice with MBPAc5-18. When MBPAc5-18-specific hybridomas were screened for the ability to respond to whole MBP as well as MBPAc5-18, only 2/29 hybridomas reacted to both whole MBP and peptide. Of the other 27 hybridomas, 7 responded to only MBPAc5-18 and 20 responded to MBPAc1-18 and MBPAc5-18. The majority of these hybridomas could represent B-type T cells that respond to peptide antigen loaded on class II MHC molecules in a different conformation than would be presented by MHC loaded with peptides processed from whole protein (80, 81, 86). The MBPAc5-18-specific hybridomas that could respond to whole MBP were fairly insensitive to antigen, requiring 1-10 μM MBPAc5-18 to stimulate IL-2 production. This is a much higher dose compared to the 10 nM MBP121-140 peptide needed to stimulate an MBP121-140-specific T cell hybridoma, even though both MBP121-140 and MBPAc5-18 bind well to

I-A^u. Together these data suggest that MBP5-16-specific T cells may be subject to tolerance in mice deficient in classic-MBP because T cells able to respond to whole MBP are only rarely detected and are low affinity (as measured by antigen responsiveness). It is possible that tolerance is mediated by MBP5-16 processed from the BG21 golli-MBP isoform that is present in $MBP^{-/-}$ mice. This hypothesis would need to be tested using mice lacking both classic and golli-isoforms of MBP.

MBPAc5-18 specific, whole MBP-responsive T cell hybridomas were used to identify residues within MBPAc5-18 that were important T cell receptor contacts. Potential TCR contact residues were mutated within MBP5-16 and the analogue peptides were used in hybridoma stimulation assays with two of the hybridomas. Hybridoma responses to wild-type and mutant MBP5-16 Q8A, R9S and K11S peptides were compared using subclones from two different hybridomas (two stable subclones were obtained from one hybridoma and only one stable subclone was obtained from the other). All three subclones had markedly decreased responses to the Q8A and K11S mutant peptides indicating that these residues are T cell receptor contacts. The R9S mutation had no effect on hybridoma proliferation as compared to wild-type 5-16 in two of the subclones derived from the same hybridoma (Figure 8 top) and was only slightly affected in the subclone from the other hybridoma (Figure 8 bottom). These data are interesting in light of the sequence differences between the N-termini of rat and mouse MBP. Rat MBP is identical in sequence to mouse MBP in MBPAc1-18 with the exception of a histidine and glycine insertion between R9 and S10 of mouse MBP. Therefore, the TCR contacts for mouse MBP5-16 are different than in rat MBP5-16. This could explain why rat MBP is able to elicit a rat MBP5-16-specific T cell response in mice while the TCR repertoire to mouse MBP5-16 is tolerized via different TCR contacts if mouse MBP5-16 is indeed tolerogenic.

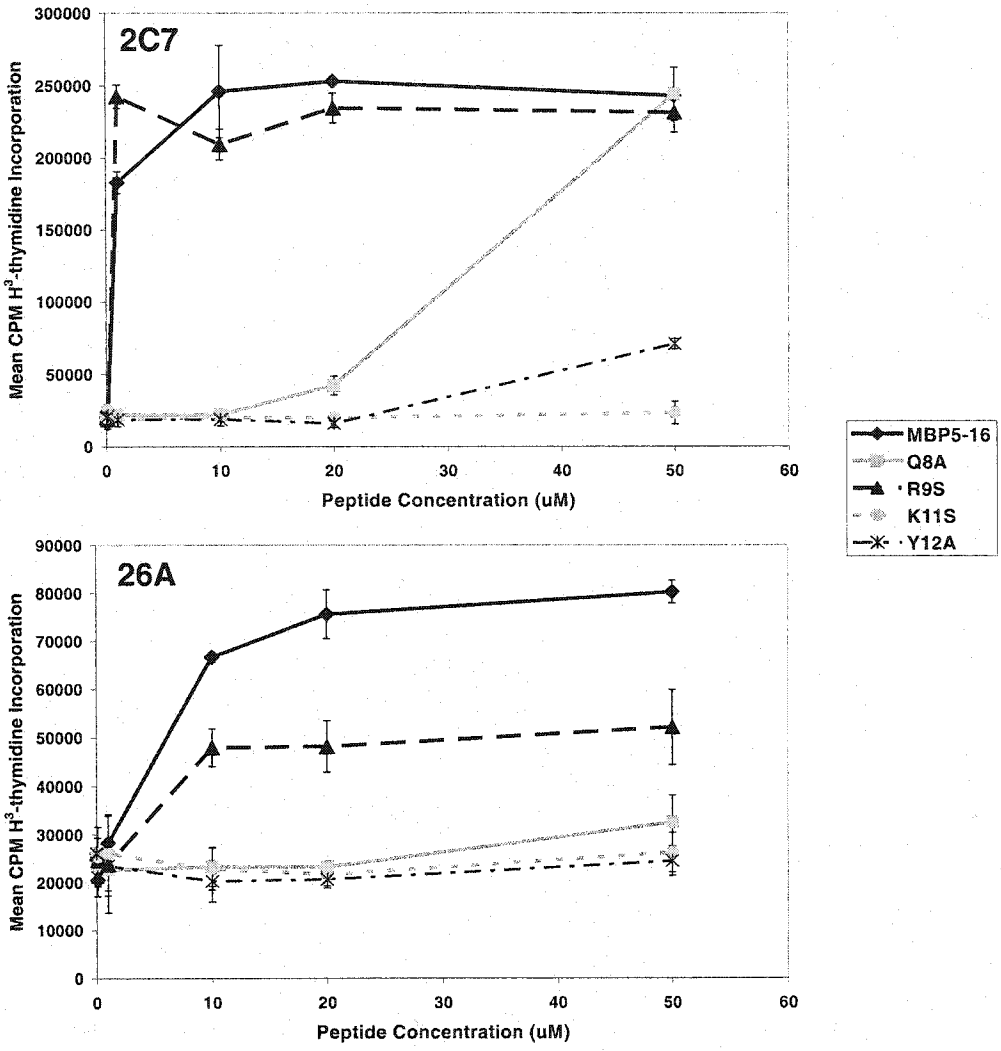

Figure 8. TCR contacts of the MBP5-16 register. Three different MBPAc5-16-specific T cell hybridomas that also respond to MBP and MBPAc1-18 were used to analyze potential TCR contacts within MBP5-16. Potential TCR contacts (see Figure 6A) were substituted in analogue peptides and dose response curves of each peptide were analyzed. The 2C7 and 2A2 hybridomas behaved similarly to all peptides (2C7 is shown). The 26A hybridoma was also similar but its responses to the R9S mutation were half maximal compared to wild-type. Doses were at 50, 20, 10, 1, 0.1 and 0 μM. Error bars are one standard deviation of triplicate wells.

Part B. MBP-specific T Cell Stimulation by APC Subsets Presenting MBP Epitopes

Introduction

Although our processing studies employed T-depleted splenocytes as APCs for MBP processing, not all splenic APCs may actually be able to present and/or stimulate T cells *in vivo* with endogenously derived MBP. Distinct APC subsets have different abilities to process and present antigen from various sources (35, 87) and have also been associated with different abilities to stimulate and regulate T cell responses (88, 89). Identification of APC subsets able to present MBP and stimulate MBP-specific T cells *in vivo* would require the use of antibodies specific for MBP peptide/I-A^u complexes, reagents that do not exist at this time. However, previous studies (61) as well as the MBP processing data described in Part A of this chapter indicated that peptides bound in the MBP5-16 and MBP125-135 registers form very stable complexes on the surface of APCs. This suggested that T cells from MBP121-150-specific TCR Tg mice might be able to detect MBP125-135/I-A^u complexes on APCs isolated directly *ex vivo*, allowing us to identify the type of APC able to present endogenously derived MBP epitopes to MBP-specific T cells.

B Cells and Dendritic Cells Constitutively Present MBP Epitopes In Vivo

Bulk mononuclear cells from the spleen and various lymph nodes were tested for their ability to stimulate MBP121-150-specific Tg T cells *in vitro* without the addition of exogenous MBP. Naïve MBP121-150-specific T cells isolated from $MBP^{-/-}$ TCR Tg mice proliferated in response to irradiated whole splenocytes, pooled brachial, axial and inguinal lymph node cells as well as to superficial and deep cervical lymph node cells isolated from wild-type B10.PL mice but not to cells isolated from $MBP^{-/-}$ mice. Interestingly, the amount of T cell proliferation induced by the various lymphoid tissues varied from mouse to mouse. Figure 9 shows the increase in T cell proliferation (stimulation index) when stimulated by mononuclear cells isolated from $MBP^{+/+}$ versus $MBP^{-/-}$ lymphoid tissues. Each point represents the stimulation index of T cells incubated

with cells from the designated tissue isolated from a single mouse. The observed differences in stimulation may reflect variation in numbers of cells that have processed MBP and are able to stimulate naïve MBP121-150-specific Tg T cells in the tissue which will be influenced by variation in the amount of MBP available to antigen presenting cells. Differences may also arise from variation in the expression of co-stimulatory molecules in tissues of individual mice. Although splenocytes were not as stimulatory as lymph node cells, both tissues were used to fractionate subtypes of APCs in order to increase the yield of dendritic cells and macrophages in experiments described below.

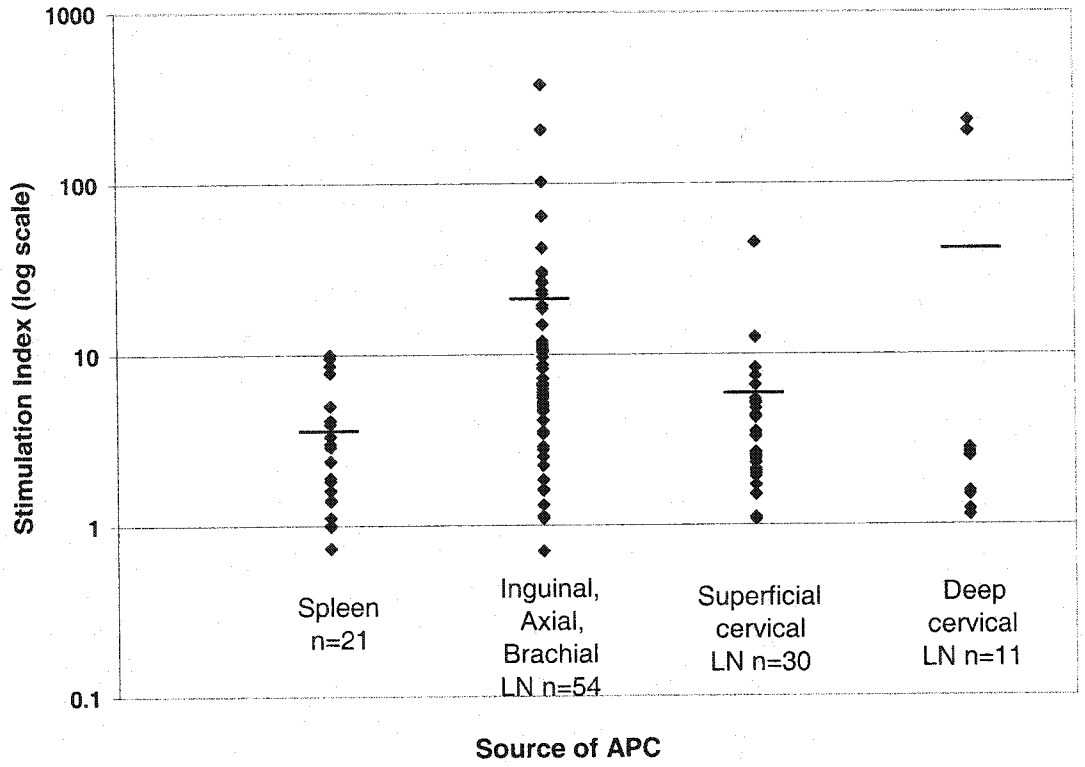

Figure 9. Variation in the ability of cells isolated from different lymphoid tissues to stimulate naïve MBP121-150-specific T cells. Single cell suspensions from different lymph nodes and spleen of 54 different B10.PL $MBP^{+/+}$ mice were irradiated and plated at $1x10^6$ cells/well in the presence of $5x10^4$ purified naïve MBP121-150-specific Tg T cells. Mice were analyzed in nine different experiments. Specific proliferation is plotted (one diamond/mouse) on a log scale as a stimulation index which was calculated by dividing the mean CPM in wells containing $MBP^{+/+}$ APCs by the mean CPM of the APCs derived from the same tissue of $MBP^{-/-}$ mice. Black bars indicate the mean stimulation index for each tissue. Statistics: tissue (average, standard deviation, median, fraction of individual samples with SI>2); spleen (3.6, 2.9, 2.9, 12/21), inguinal, axial, brachial LN (22.6, 58.6, 6.1, 46/54), superficial cervical LN (5.5, 8.0, 3.4, 24/30), deep cervical LN (41, 87, 2.6, 7/11).

To define the subtype of APC that presents antigen to naïve MBP121-150-specific Tg T cells, splenocytes from $MBP^{+/+}$ and $MBP^{-/-}$ mice were fractionated using autoMACS separation and cell sorting based on the expression of B220, CD11c and F4/80. Purified populations were used to stimulate naïve MBP121-150-specific Tg T

cells. As shown in Figure 10 (left panel), only the $CD11c^+$ population triggered significant proliferation, indicating that dendritic cells are the major cell type able to present endogenously-derived MBP121-150 epitopes to naïve Tg T cells.

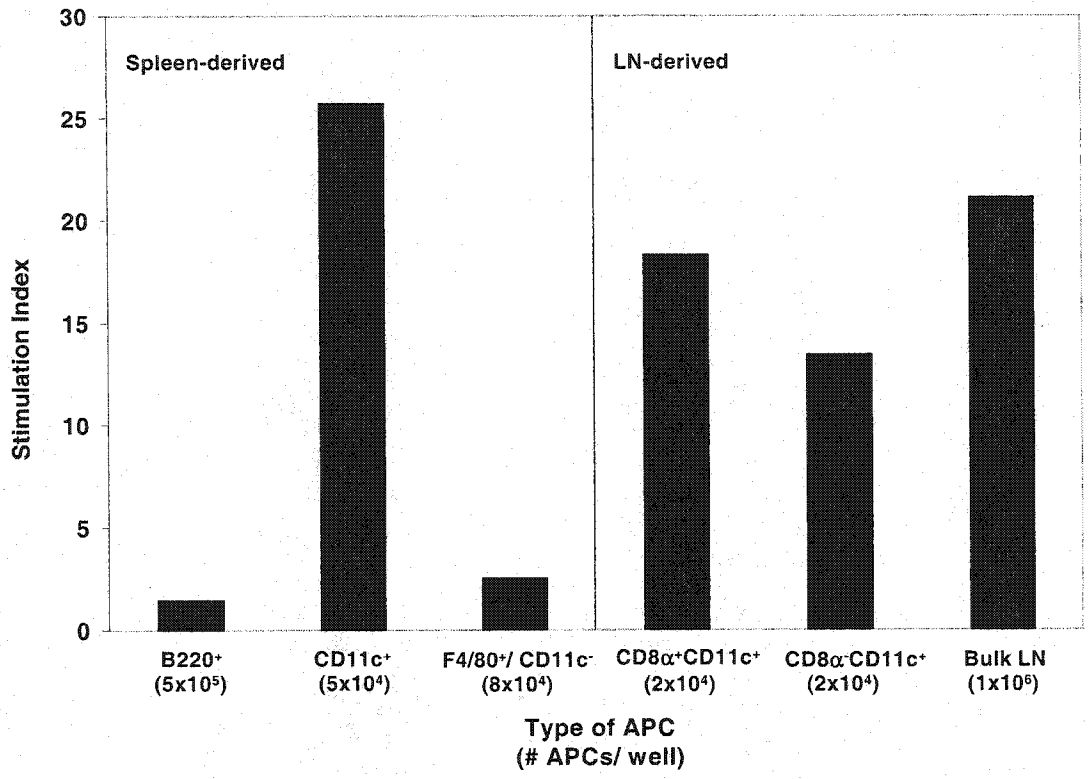

Figure 10. Naïve MBP121-150-specific Tg T cells are stimulated by two subsets of dendritic cells ex vivo. Proliferation (^{3}H-thymidine incorporation) of purified MBP121-150 specific Tg T cells was used to detect endogenously derived antigen on APC subsets. APCs were isolated from B10.PL MBP$^{+/+}$ and MBP$^{-/-}$ mice. Purified Tg T cells (6x10^4/well) were added to 96 well plates with the number of APCs indicated in the graph. In the left panel, APCs were isolated from spleen suspension cultures (non-collagenase digested). B220$^+$ cells were purified using autoMACS. CD11c$^+$ and F4/80$^+$/CD11c$^-$ cells were obtained by cell sorting T and B cell depleted (autoMACS) splenocytes. The left panel is representative of two experiments. In the right panel (one experiment), collagenase-digested peripheral lymph nodes (LN) were used to isolate CD8α$^+$ and CD8α$^-$ DCs. Lymph node cells were enriched for DCs by depleting T and B cells and were then sorted based on CD8α expression. Purity of sorted cells in this experiment was not optimal (cells were > 79% pure in all samples) but contaminants were mostly small, non-CD11c$^+$ cells. Both subsets present MBP121-150 epitopes to naïve T cells. Data is shown as a stimulation index that was calculated by dividing the mean CPM in wells containing MBP$^{+/+}$ APCs by the mean CPM in wells containing MBP$^{-/-}$ APCs.

Different subsets of dendritic cells have been associated with different functions in regards to T cell regulation, T cell polarization and cross-presentation (90). In order to determine if there are differential abilities of DC subsets to stimulate naïve MBP121-150-specific T cells, we subfractionated DCs based on CD8α expression. Three experiments were done using various methods. $CD8\alpha^+$ and $CD8\alpha^-$ DC subsets from both spleen and lymph nodes were examined because bulk lymph node cultures stimulate Tg T cells better than splenocytes and because there are different types of DCs within the $CD8\alpha^+$ and $CD8\alpha^-$ subsets of lymph node DCs compared to the $CD8\alpha^+$ and $CD8\alpha^-$ subsets in the spleen. Figure 10 (right panel) shows one experiment in which DCs were isolated from collagenase-digested axial, inguinal, brachial and superficial cervical lymph nodes and sorted based on CD8α expression. Both $CD8\alpha^+$ and $CD8\alpha^-$ DCs were able to stimulate naïve MBP121-150-specific Tg T cells (Figure 10, right panel). Although the purity was not optimal in the experiment shown in Figure 10, two additional experiments performed in different ways demonstrated that both $CD8\alpha^+$ and $CD8\alpha^-$ DC populations were able to stimulate naïve MBP121-150-specific Tg T cells. These other experiments included 1) isolation of DCs from non-collagenase digested spleen (data not shown) and 2) removing DC subsets from collagenase digested lymph node cells via cell sorting (Figure 11). In the latter experiment, MBP121-150-specific Tg T cells proliferated to whole lymph node cells as well as to lymph nodes depleted of either DC type ($CD8\alpha^+$ DC-depleted or $CD8\alpha^-$ DC-depleted lymph node cells) but proliferated only slightly to lymph node cells depleted of all $CD11c^+$ cells (Figure 11). This experiment verified that $CD11c^+$ cells are the main cell type able to stimulate naïve MBP121-150-Tg T cells in lymph nodes (this had only been demonstrated in spleen in previous experiments).

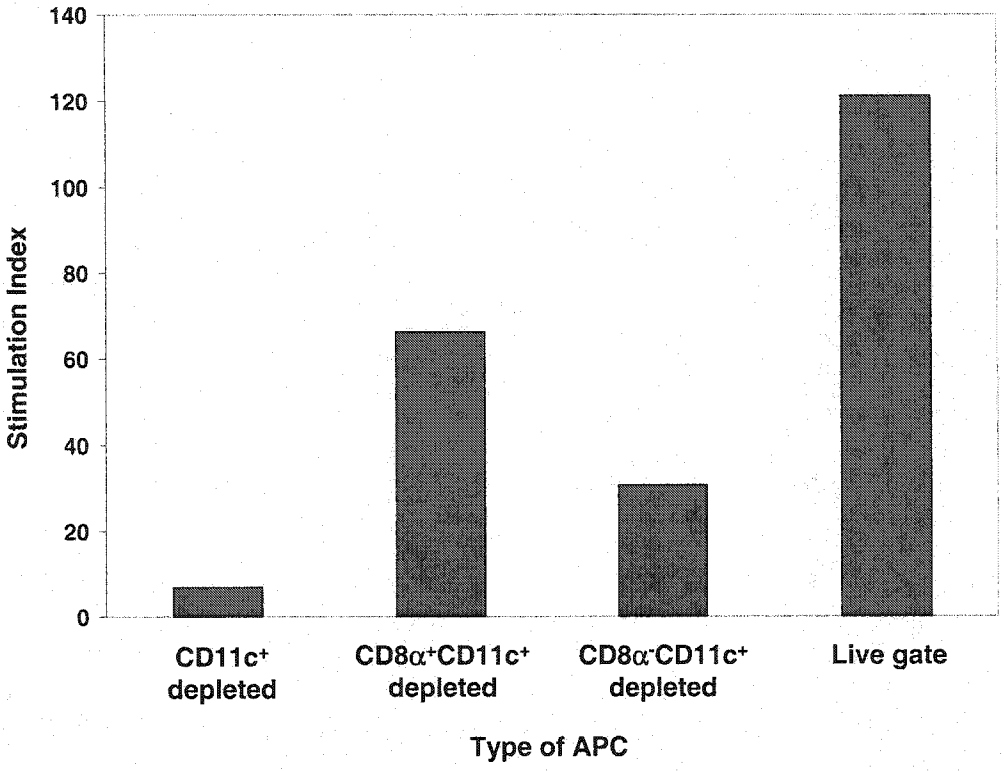

Figure 11. DCs are the primary APCs that stimulate naïve MBP121-150-specific Tg T cells in lymph nodes. APCs were isolated from collagenase-digested peripheral lymph nodes of either $MBP^{+/+}$ or $MBP^{-/-}$ mice. $CD11c^+$, $CD8\alpha^+CD11c^+$ or $CD8\alpha^-CD11c^+$ cell populations were removed by sorting. Cells were also sorted through a live gate for a positive control. Sorter cells were irradiated and then plated at $1x10^6$ cells/well. Purified naïve MBP121-150-specific Tg T cells were added at $6x10^4$/well. Data is presented as the stimulation index calculated as described in Figure 10.

Our data implicate dendritic cells as the major cells that can stimulate naïve MBP-121-150 Tg T cells. The initial interaction between the naïve T cell and DC is important in determining development of tolerance versus disease, but DCs may not be the only APCs that process and present MBP epitopes. We therefore fractionated collagenase-digested spleen and lymph node cells into different APC subsets and incubated them with naïve and *in vitro* activated MBP121-150 Tg T cells. While naïve Tg T cells proliferated in response to DCs and not to B cells, activated Tg T cells were able to respond to both

DCs and B cells (Figure 12). Interestingly, the activated T cell response to lymph node B cells was 21 times higher than naïve T cells while the activated T cell response to splenic B cells was only four-fold better than naïve cells (Figure 12). These data suggest that endogenously derived MBP epitopes are processed and presented by both B cells and dendritic cells but only previously activated T cells are able to recognize and respond to MBP presented by B cells.

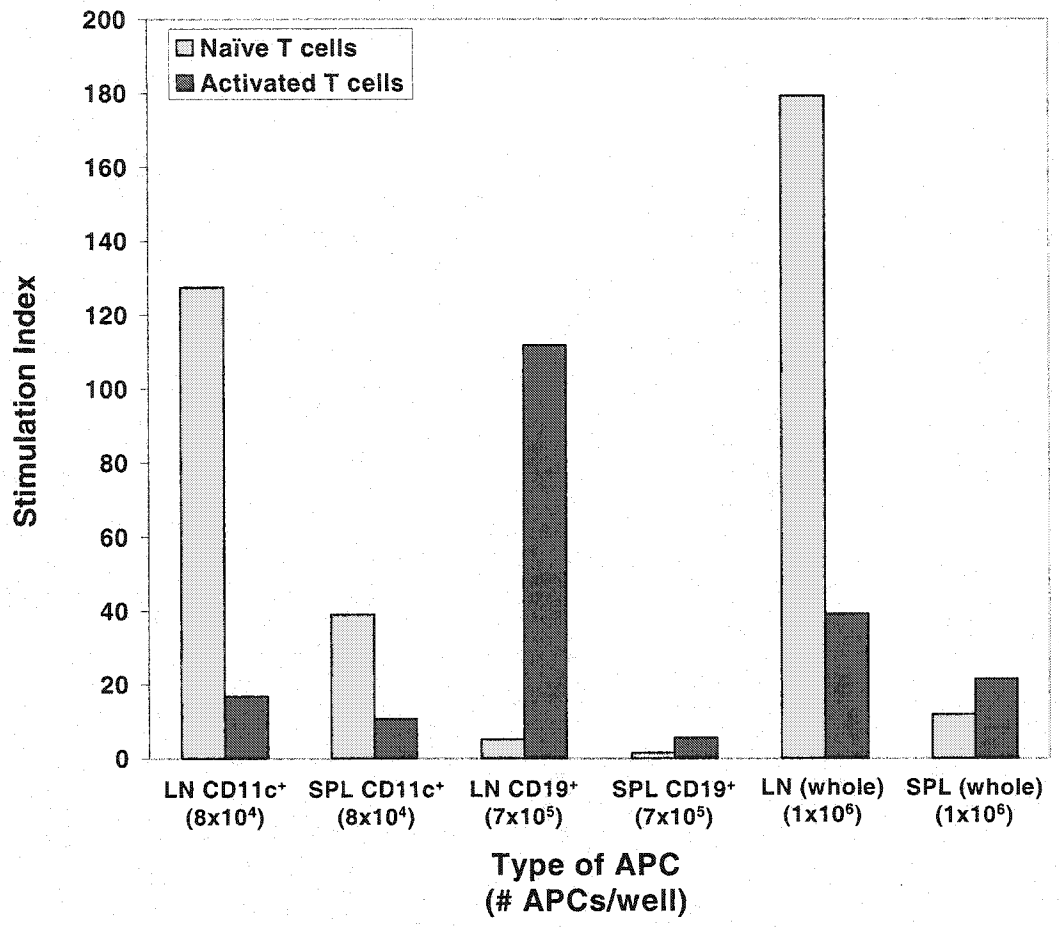

Figure 12. MBP epitopes are presented by both DCs and B cells. Naïve and *in vitro* activated MBP121-150-specific Tg T cells ($8x10^4$/well) were incubated with collagenase-digested lymph node (LN) or spleen (SPL)-derived $CD11c^+$ DCs, $CD19^+$ B cells and whole LN or SPL. Purity of DC and B cell populations used was greater than 92%. Data is shown as a stimulation index which was calculated by dividing the mean CPM in wells containing $MBP^{+/+}$ APCs by the mean CPM of wells containing $MBP^{-/-}$ APCs. Data shown is from one experiment.

Discussion (Part A and B)

We identified I-A^u-restricted peptides that are generated from processing of whole MBP by B10.PL mouse APCs. The most abundant MBP peptides eluted from I-A^u are MBPAc1-17 and MBPAc1-18. A second set of nested peptides containing the core MBP125-135 was found at much lower abundance. The observation that more N-

terminal than MBP125-135 peptides are presented on the cell surface of APCs is the opposite of what we predicted from our T cell tolerance studies. This paradox is explained by the demonstration that MBPAc1-18 binds to I-A^u using two distinct binding registers, MBPAc1-11 and MBP5-16. The biphasic dissociation kinetics of MBPAc1-18 and the dissociation rates of analogue peptides shown in Figure 6 indicate that most of the MBPAc1-17 and MBPAc1-18 peptides are bound in the MBP5-16 register. The truncated N-terminal peptides generated by processing that lack the acetyl group and first few amino acids of the protein (Table 1) must also be bound in the MBP5-16 register because they lack important residues required for binding in the MBPAc1-11 register (91). MBPAc1-11-specific T cells do not recognize N-terminal peptides bound in the MBP5-16 register and therefore, even in the presence of abundant N-terminal peptides, do not encounter sufficient ligand to undergo tolerance induction.

The demonstration that all N-terminal peptides generated by processing intact MBP contain the MBP5-16 binding register differs from conclusions reported by Fairchild et al. (84). These investigators described the MBP5-16 I-A^u binding register as "absolutely cryptic", i.e. peptides bound in this binding register are never generated by processing the intact protein (84). This conclusion was reached in part because MBP5-16-specific T cells were not detected in H-2^u mice immunized with spinal cord homogenate. However, as noted by these investigators, this result could be due to T cell tolerance induced by APCs presenting peptides bound in the MBP5-16 register. This idea is consistent with our results indicating that N-terminal peptides bound in the MBP5-16 register were more abundantly eluted from I-A^u than the highly tolerogenic MBP125-135 peptides. MBP5-16 was also considered cryptic because MBPAc1-11 specific T cell hybridomas did not respond *in vitro* to peptides longer than MBPAc1-13 on fixed APCs (84). This result suggested that processing is required to remove the MBP5-16 register in order for these peptides to be recognized by MBPAc1-11-specific T cells. In contrast, we demonstrate that T cells expressing two different Tg MBPAc1-11-specific TCRs respond well to MBPAc1-18 presented on fixed APCs. This difference may be due to increased

sensitivity of the Tg T cells used in our experiments compared to the T cell hybridomas used in earlier experiments (84).

It was initially surprising that the nested set of peptides containing MBPAc1-17 and MBPAc1-18 were approximately 23 times more abundant than the MBP125-135 nested set of peptides because all of these peptides exhibit similar affinities for I-A^u. Several factors may account for the higher abundance of N-terminal peptides in the repertoire of MBP peptides eluted from I-A^u. Alternative splicing that generates the most abundant isoform of murine MBP (14 kDa isoform), as well as the 17.2 kDa isoform, includes the N-terminal region but excludes the region containing MBP125-135 (26), resulting in a five-fold enrichment of N-terminal sequences in MBP purified from myelin. Additionally, the ends of a protein may be more likely to denature and easier to process than sequences in the middle of the protein. Lastly, the N-acetyl group may inhibit exopeptidase activity and protect these peptides from further degradation. This is consistent with the observation that non-acetylated peptides in the MBPAc1-18 nested set are detected at comparable levels to the MBP125-135 peptides (Table 1) while MBPAc1-17 and MBPAc1-18 are more abundant.

We used sequence-specific methodology to identify the two nested sets of peptides generated from whole MBP processing. Therefore, these two nested sets may not be the only two sets generated from processing whole MBP. Masses of peptides centered around previously identified MBP T cell epitopes (MBPAc1-11, MBP125-135 and MBP136-146) were used to specifically screen the data set obtained from subtractive analysis of the FT-ICR-MS data. In order to identify I-A^u-restricted MBP peptides that have not been identified as T cell epitopes, we would need to either 1) screen the data set for masses of all peptides that could possibly be processed from whole MBP or 2) identify candidate I-A^u binding motifs within MBP and screen our data set for peptides centered around the candidate motifs. The first option, if automated, would be the most systematic method to identify additional peptides processed from whole MBP.

The competition for binding to I-A^u between the MBPAc1-11 and MBP5-16 binding registers is a likely explanation for the lack of tolerance induction in MBPAc1-

11-specific T cells. The bias toward the amount of peptide bound in the MBP5-16 register that was observed *in vitro* following a one hour incubation of MBPAc1-18 with soluble I-A^u may be even stronger *in vivo* because increasing the incubation to 16 hours increased the percentage of peptide bound in the MBP5-16 register. The one-hour incubation time could be an underestimate of the length of time that I-A^u is exposed to MBP peptides *in vivo*. One study indicated that there is approximately a twelve hour delay before peptide derived from endocytosed protein is processed and presented on the surface of activated dendritic cells *in vitro* (92). However, Jenkins and coworkers detected processed antigen in draining lymph nodes as early as four hours after a subcutaneous injection of whole antigen that drained to the lymph nodes within 30 minutes (93). Variation in processing time is likely to be protein and antigen dependent. H-2M activity may also influence which register is utilized in complexes containing MBPAc1-18 and I-A^u on the cell surface and it is likely to favor the more energetically stable MBP5-16 register (94-96).

The observation that a tolerogenic MBP epitope can be detected by naïve Tg T cells directly *ex vivo* only when presented by dendritic cells provides experimental confirmation of the dominant role believed to be played by these APCs in maintaining tolerance to auto-antigens. However, our data do not implicate a specific subtype of DC in maintaining peripheral tolerance to $CD4^+$ MBP-specific T cells. In mice, there are at least six subtypes of DCs that have been associated with different functions such as generation of Th1 versus Th2 inflammatory responses, production of IFN-α in response to viruses, tolerance induction (88, 90) and generation of regulatory T cells (97). However, the correlation of phenotype with function is difficult due to the plastic nature of DCs as well as differences in the types of responses being investigated and how the DCs are isolated/cultured. One of the major cell surface markers used to separate DC subsets is CD8α. $CD8\alpha^+$ and $CD8\alpha^-$ DCs are generally $CD11b^-$ and $CD11b^+$, respectively. Three subsets of $CD8\alpha^+$ and $CD8\alpha^-$ DCs that are found in lymph nodes and spleen (the third subset is further differentiated by CD4 expression in $CD8\alpha^-$ DCs), are thought to enter these organs through the blood. These DCs therefore have been

designated as "blood-derived" DCs (88). Another $CD8\alpha^-$ subset is present in lymph nodes only and appears to enter lymph nodes from tissues via lymphatics. Skin-draining lymph nodes contain this "tissue derived" $CD8\alpha^-$ subset as well as $CD8\alpha^{lo}$ Langerhan's DCs that migrate to lymph nodes from the skin (98, 99).

Different DC subtypes have been associated with differential abilities to capture and present various sources of antigen to naïve T cells (88, 90). However, most *in vivo* studies that describe the phenotype of the antigen presenting DCs have involved the administration of labeled exogenous antigen (either soluble or particulate) via subcutaneous or intravenous injection (93, 100-102). Although these studies may not be completely relevant to the presentation of self-antigens in a non-manipulated environment, they do demonstrate differences in the abilities of DC subtypes to present different types of antigens given at different locations or routes (93, 100-102).

Studies regarding processing and presentation of endogenously-derived self-antigens have been less definitive because of the lack of methods other than T cell assays to detect antigen presentation. In one study, Scheinecker et al. demonstrated that naïve T cells specific for H^+K^+-/ATPase expressed by gastric parietal cells could be stimulated by both $CD8\alpha^+$ and $CD8\alpha^{lo}$ DCs isolated from gastric lymph nodes *ex vivo*. Fluorescent immunohistochemistry also demonstrated that both $CD11b^+$ and $CD11b^-$ (as well as $CD8\alpha^+$ and $CD8\alpha^-$) DCs contained intracellular H^+K^+-/ATPase in gastric lymph nodes but only $CD11b^+$ and not $CD8\alpha^+$ DCs could be found adjacent to gastric parietal cells in the stomach (103). In contrast, another study demonstrated that only $CD11b^+$ and not $CD11b^-$ DCs from pancreatic lymph nodes were able to present islet antigens to $CD4^+$ T cells *ex vivo* (104).

We separated DCs based on CD8α expression in order to investigate whether these subsets had differential abilities to stimulate naïve MBP-specific Tg T cells *ex vivo* that would indicate different roles in MBP-specific tolerance induction. Both spleen and lymph node derived $CD8\alpha^+$ and $CD8\alpha^-$ DCs stimulate naïve MBP121-150-specific Tg T cells *ex vivo*, indicating that for MBP-specific $CD4^+$ T cells, multiple DC subtypes are potentially involved in maintaining tolerance. Lymph node cells from individual mice

tend to stimulate naïve Tg T cells more than splenocytes (Figure 9). It is possible that "tissue-derived" DCs, which have higher expression of MHC class II molecules (98, 99) and are not present in the spleen, are responsible for the increased proliferation of naïve Tg T cells seen *ex vivo*. It is also possible that lymph nodes that drain tissues innervated with myelinated axons may contain more free or cell-associated MBP than the spleen. However, in lymph nodes, we were not able to distinguish whether "tissue-derived" or "blood-derived" (or both) DCs stimulate naïve Tg T cells *ex vivo* in these experiments.

Although DCs were the only APC subset able to stimulate naïve MBP-specific Tg T cells, other APC subsets may also present MBP epitopes but are unable to stimulate naïve T cells due to inadequate co-stimulation. Therefore, activated MBP121-150-specific Tg T cells were used to investigate whether B cells or macrophages also present MBP epitopes. In addition to DCs, we expected that macrophages would also present MBP121-150 because of their ability to pick up exogenous proteins and particulate matter in a non-antigen specific manner. However, because of technical difficulties, we were unable to obtain pure macrophage populations in experiments using activated Tg T cells and cannot say for certain if macrophages present MBP peptides. Surprisingly, we found that $CD19^+$ B cells from unmanipulated wild type mice were able to stimulate activated but not naïve MBP121-150-specific Tg T cells, while DCs were able to stimulate both naïve and activated Tg T cells. Interestingly, lymph node B cells provided better stimulation of activated Tg T cells than splenic B cells on a per cell basis. Purification of B cells with anti-B220 demonstrated similar results with activated Tg T cells however, we did not use naïve Tg T cells as a comparison in that particular experiment (data not shown). The observation that B cells present endogenously derived MBP to Tg T cells *in vivo* is intriguing. Purified B cells incubated with exogenously added whole MBP *in vitro* will stimulate naïve Tg T cells (data not shown) indicating that they can take up, process and present MBP. However, MBP concentrations in *in vitro* experiments are presumably much higher than will be encountered *in vivo* and this *in vitro* presentation may not represent B cell receptor (BCR)-mediated internalization, which is thought to be necessary for efficient antigen internalization and presentation by

B cells. Assuming B cells take up MBP in a BCR-specific manner, it is surprising that there are enough B cells with MBP-specific BCRs in spleen and lymph nodes of unprimed, unmanipulated mice to stimulate activated MBP-specific T cells *ex vivo*. It is possible that B cells present MBP in a BCR-independent fashion. There is research demonstrating that naïve B cells interact with and obtain antigen from DCs in a BCR-independent manner that they can then process and present on their own MHC class II molecules (105, 106).

We have demonstrated that both $CD8\alpha^+$ and $CD8\alpha^-$ DCs present MBP epitopes to naïve MBP121-150-specific Tg T cells and that both DCs and B cells present MBP to activated Tg T cells. Our processing experiment identified peptides that are processed from whole MBP and the relative abundances of each peptide on T cell-depleted splenocytes. One caveat to these studies is that the peptides and the peptide abundances shown from our processing study may not be representative of the results of MBP processing by individual APC subsets. Because we used T-depleted splenocytes, B cells were the primary component of the APCs used in our study, with DCs being a minor component. Processing machinery between APC subsets may be different and could result in differences in antigen processing and presentation. Lysosomal proteases are important for antigen processing and presentation in the class II MHC pathway. Additionally, many lysosomal proteases, specifically cathepsins and asparagine endopeptidase, demonstrate cell type-specific expression and activity in APC subsets and other cell types although DCs and B cells appear to have similar expression patterns of these proteases (107). Experiments demonstrating roles of specific proteases in the generation of specific antigenic peptides in APCs are limited and substantially more limited regarding antigen processing in subsets of APCs. Hsieh et al. studied the effect of cathepsin S and cathepsin L on antigen processing in a fibroblast cell line engineered to express $I\text{-}A^b$ and either cathepsin S or L. Mass spectrometry analysis of endogenous peptides on the surface of the engineered cell lines indicated that the most abundant peptides were generated independently of cathepsin S or L activity. However, cathepsin S or L were involved in the destruction or generation of a few specific peptides and

relative levels of some peptides were discordant on cells expressing cathepsin L versus cathepsin S (108) indicating that these proteases can differentially influence processing of specific peptides. The generation of specific T cell epitopes from exogenously added protein in the cathepsin S or L-expressing cell lines was also studied and patterns of antigen processing were similar to that observed for the processing of endogenous peptides (108). In another study, while HEL degradation in HEL-specific BCR Tg B cells deficient in cathepsins S, L and B was not inhibited, the generation of two specific HEL T cell epitopes but not another HEL epitope were dependent on cathepsin S (109). However, this study did not address the effect of inhibited invariant chain degradation (which occurs in the absence of cathepsin S) on the presentation of the specific HEL T cell epitopes and this could have affected presentation of these HEL epitopes. Regarding differential antigen processing and presentation by APC subsets, DiPaolo and Unanue stated that although the total amount of HEL peptides processed and presented on I-A^k differed between APC subsets (B cells, macrophages and DCs), the relative abundances of different epitopes was constant (110). For I-A^k restricted HEL epitopes presented by peripheral APCs, there may not be major differences in processing between APC subsets. This may be an antigen-specific effect and epitopes of other antigens could be processed differentially by APC subsets. Antigen processing abilities of APCs could be influenced by differences in the processing machinery between APCs, differences in antigen internalization and/or targeting to different endosomal compartments (35) or APC activation state.

If our processing data is representative of the actual MBP epitopes presented *in vivo*, then the fact that presentation of very low levels of MBP125-135 peptides by DCs to naïve T cells is sufficient to induce tolerance suggests that very little MBPAc1-17 and MBPAc1-18 is normally bound in the MBPAc1-11 register because it is not sufficient to induce tolerance in MBPAc1-11-specific T cells. However, MBPAc1-18 peptide bound in the MBPAc1-11 register is detected by activated MBPAc1-11-specific T cells *in vivo* during disease. It is interesting and perhaps important to disease that B cells from an untreated animal can stimulate activated MBP-specific T cells. We have only

demonstrated stimulation by B cells for activated MBP121-150-specific Tg T cells and have been unable to detect proliferation of naïve or *in vitro* activated MBPAc1-11-specific Tg T cells to any *ex vivo* isolated APCs, including purified DCs and B cells (data not shown). Nevertheless, *in vivo* activated MBPAc1-11-specific T cells may still be able to respond to B cells presenting N-terminal MBP epitopes. While B cells are not required for disease induction in some murine EAE models induced by active immunization (111, 112), B cells may modulate acute EAE (111) and targeted antigen presentation by B cells protects rats against active induction of EAE (113). However, antigen presentation by B cells specific for CNS proteins may contribute to an autoreactive response by specifically concentrating CNS proteins for antigen presentation to T cells and by producing anti-CNS protein antibodies that opsonize antigen for presentation by other APCs (114).

It is possible that presentation of MBP epitopes by unactivated B cells would dampen an autoimmune response by providing suboptimal levels of costimulation or by skewing the response to a Th2-type response. However, activated B cells presenting sufficient levels of MBP may enhance an autoimmune response. Factors that may enhance detection of MBPAc1-11-bound peptide during inflammation include elevated levels of all MBP epitopes due to increased MBP degradation, stimulation of activated T cells by B cells, macrophage and DCs during inflammation and increased expression of co-stimulatory molecules on APCs presenting MBP epitopes. Thus, the competition between two binding registers allows most MBPAc1-11-specific T cells to escape tolerance induction by DCs presenting self-antigen under non-inflammatory conditions but may allow MBPAc1-11-specific T cells to see sufficient amounts of their epitope under inflammatory conditions to initiate autoimmunity.

Chapter 5: Investigation of the Basis of Differences in Spontaneous EAE Incidence between Two MBPAc1-11-specific TCR Tg Mouse Lines

Introduction: Spontaneous EAE in MBP Ac1-11-specific TCR Tg Mice

Most of the MBP-specific T cells in wild-type B10.PL (H-2^u) mice are specific for a single epitope within MBP, MBPAc1-11. The studies described in Chapter 4 provide insight into how processing of MBP inhibits tolerance induction of MBPAc1-11-specific T cells. Disease can be induced in H-2^u mice by immunization with myelin antigens, but spontaneous EAE is not observed in wild-type B10.PL mice. However, if the precursor frequency of MBPAc1-11-specific T cells is significantly enhanced, as in the case of MBPAc1-11-specific TCR Tg mice, EAE develops spontaneously in a percentage of the mice.

Two independently generated lines of MBPAc1-11-specific TCR Tg mice, Tg1 (42) and Tg2 (64), both demonstrate a lack of central and peripheral tolerance of MBPAc1-11-specific T cells as there are large numbers of phenotypically naïve Tg T cells in the thymus and periphery of healthy mice. Both strains develop spontaneous EAE, but the incidence differs between the lines. In conventional housing facilities, 43% of Tg1 (70) mice and 10% of Tg2 (115) mice develop spontaneous EAE. Interestingly, if animals are housed in SPF facilities, spontaneous EAE incidence decreases to 15% (70, 115) in the Tg1 mice, indicating that microbial exposure facilitates the development of spontaneous EAE. Incidence in Tg2 mice remains the same in SPF facilities (T. Brabb and J. Goverman, unpublished observations). The basis for these differences in spontaneous EAE incidence in two TCR Tg lines with the same T cell specificity is unclear. Possible explanations include: 1) the Tg1 TCR may be more cross-reactive to environmental antigens than the Tg2 TCR, 2) differences in affinities between the two TCRs might make Tg1 T cells more sensitive to stimulation by endogenous MBP peptide/MHC complexes than Tg2 T cells, 3) differences in affinities between the two TCRs may also influence the cytokine milieu produced by the two types of T cells and 4) there could be differences in the generation, maintenance, function and trafficking of

regulatory T cells between the two strains. Song et al. showed that there are increased numbers of Tg1 T cells in the gut and gut associated lymphoid tissues (GALT) compared to Tg2 T cells (116). Additionally, Tg1 T cells are more activated in Peyer's patches (determined by CD69 and CD45RB staining) (116) and mesenteric lymph nodes (CD44 and CD45RB staining) compared to Tg2 cells (117). Increased activation in GALT could be indicative of increased cross-reactivity to environmental antigens by Tg1 T cells compared to Tg2 T cells or due to decreased T cell regulation in the gut between the strains. There is some evidence suggesting that Tg1 T cells produce more IFN-γ upon stimulation with MBPAc1-11 than Tg2 T cells, which produce more IL-4 and TGF-β (117). However, in these studies it was not clear that Tg T cells were responsible for cytokine production because cytokine positive cells were detected via ELISPOT and were not identified as T cells by cell surface staining.

In order to investigate possible explanations for the differences in spontaneous EAE incidence between the MBPAc1-11-specific Tg1 and Tg2 strains, we compared *in vitro* proliferative and intracellular cytokine responses of T cells isolated from each strain. We hypothesized that there are differences in proliferation and cytokine production between T cells of the Tg lines when stimulated. W also hypothesized that the two strains might differ in their ability to respond specifically to processed whole MBP but not to the MBPAc1-11 peptide. Therefore, we analyzed T cell responses to both whole MBP and peptide stimulation.

In Vitro Proliferative Responses of MBPAc1-11-specific Tg1 and Tg2 T Cells are Similar

To study proliferative responses of Tg1 and Tg2 T cells to whole MBP, MBPAc1-18 and MBPAc1-11, we used *in vitro* proliferation assays in which we attempted to equalize the number of Tg T cells in each well between the strains. Because there is no commercially available antibody to the TCR Vα gene expressed in Tg2 T cells (Vα4), equal numbers of Vβ8.2$^+$ Tg1 and Tg2 T cells were compared in the proliferation assays. Tg T cells were isolated using positive selection of Vβ8.2$^+$ cells and equal numbers of

Vβ8.2$^+$ T cells and irradiated APCs were added to each well and stimulated with whole MBP, MBPAc1-18 or MBPAc1-11. Interestingly, while both Tg1 and Tg2 T cells proliferated similarly to both MBPAc1-18 and MBPAc1-11, purified Tg2 T cells did not respond to whole MBP (Figure 13). The same effect was seen in cells purified using anti-CD4 antibody. However, this effect is apparently an artifact due to the positive purification of Tg2 cells because experiments using unpurified RAG$^{-/-}$ Tg1 or Tg2 splenocytes revealed no difference in the proliferative response of cells from both Tg lines to whole MBP, MBPAc1-18 and MBPAc1-11. Similar results were also obtained with cells purified via negative selection for CD4$^+$ T cells (Figure 14). It is not clear why positive purification affected only Tg2 T cell responses to whole MBP.

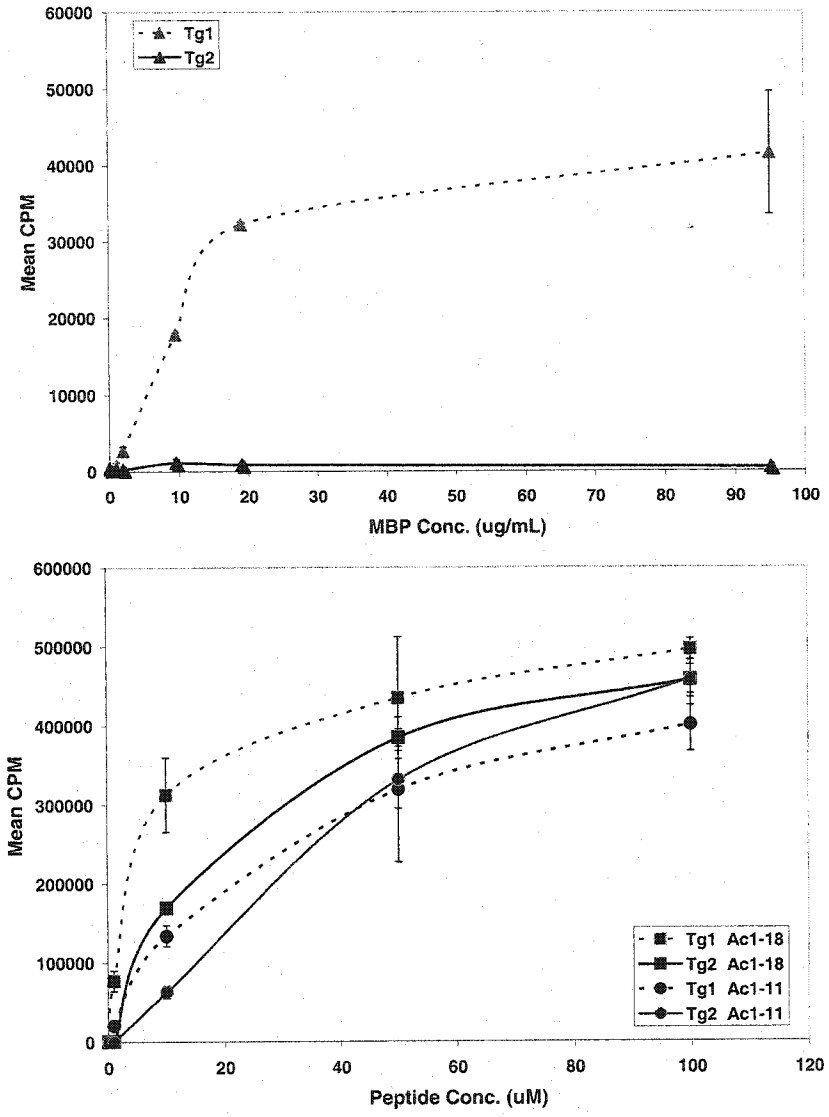

Figure 13. Different proliferative responses of MBPAc1-11-specific Tg T cells purified using anti-Vβ8.2 and AutoMACS cell separation to whole MBP. Naïve T cells purified from Tg1 or Tg2 MBPAc1-11-specific TCR Tg lines (Tg1, dotted lines; Tg2, solid lines) using autoMACs cell separation and anti-Vβ8.2 antibody were plated in the presence of $1x10^6$ irradiated APCs and the indicated concentrations of MBP (top panel) or peptide (Ac1-18 or Ac1-11; bottom panel). Responses to MBP, MBPAc1-18 and MBPAc1-11 are indicated by solid triangles, squares and circles, respectively. Error bars are one standard deviation of counts from triplicate wells. Similar results were seen using T cells purified with anti-CD4 antibody.

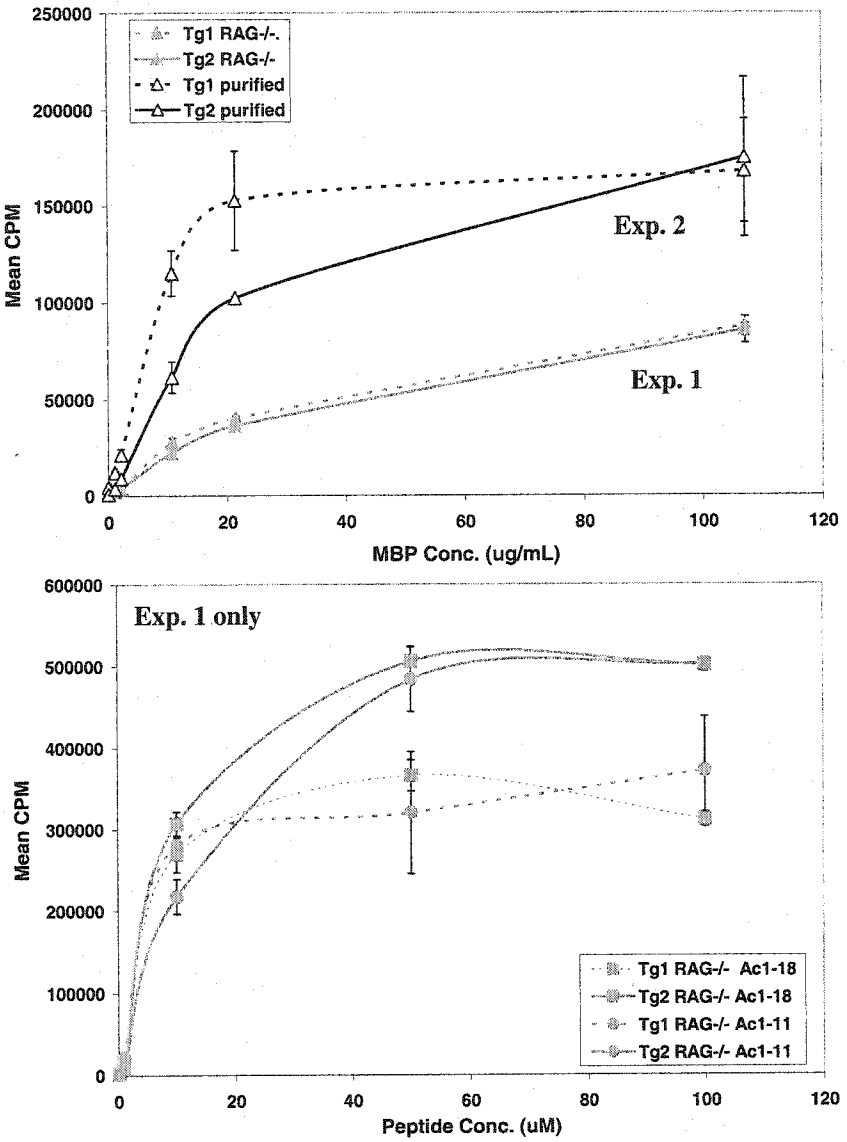

Figure 14. Unpurified or CD4⁺ T cells purified by negative selection on the AutoMACS from Tg1 and Tg2 lines are both able to respond to whole MBP and peptides. The top panel shows two different experiments (Exp. 1 and Exp. 2). Unpurified Tg1 and Tg2 cells from RAG$^{-/-}$ TCR Tg mice (grey lines, filled triangles) in experiment one and CD4^{+} Tg1 and Tg2 T cells purified via negative selection (black lines, open triangles) in experiment 2 were incubated with $1x10^{6}$ irradiated APCs and whole MBP. The bottom panel shows dose response of unpurified Tg1 and Tg2 (from RAG$^{-/-}$ mice) only. Cells that were negatively purified responded similarly (data not shown). Tg1 T cells, dotted lines; Tg2 T cells, solid lines; MBPAc1-18, squares; MBPAc1-11, circles. Error bars are one standard deviation of counts from triplicate wells.

Differences in Cytokine Production by MBPAc1-11-specific Tg1 and Tg2 T cells

T cell proliferation is only part of a T cell response and the proliferative response is not always coupled to cytokine production (118). It is possible that there are differential cytokine responses between Tg1 and Tg2 T cells stimulated with antigen. We analyzed intracellular cytokine production in both Tg1 and Tg2 T cells stimulated with either whole MBP or MBPAc1-11. Cytokine production was analyzed for both naïve and previously activated Tg T cells.

We performed two time-course experiments analyzing intracellular cytokines produced by naïve (Figure 15) and activated (Figure 16) Tg1 and Tg2 T cells. To obtain direct comparisons of Tg1 and Tg2 T cells, we purified naïve T cells from Tg1 and Tg2 mice using a negative selection $CD4^+$ T cell enrichment kit. Purified T cells were then either 1) stimulated to analyze T cell cytokine production of naïve cells or 2) cultured with MBP or MBPAc1-11 and APCs for 7 days and then stimulated a second time for cytokine analysis. $Thy1.1^+$ APCs were used so that we could use anti-Thy1.2 and anti-CD4 antibodies to identify transgenic T cells even if TCR chains are down-regulated upon activation.

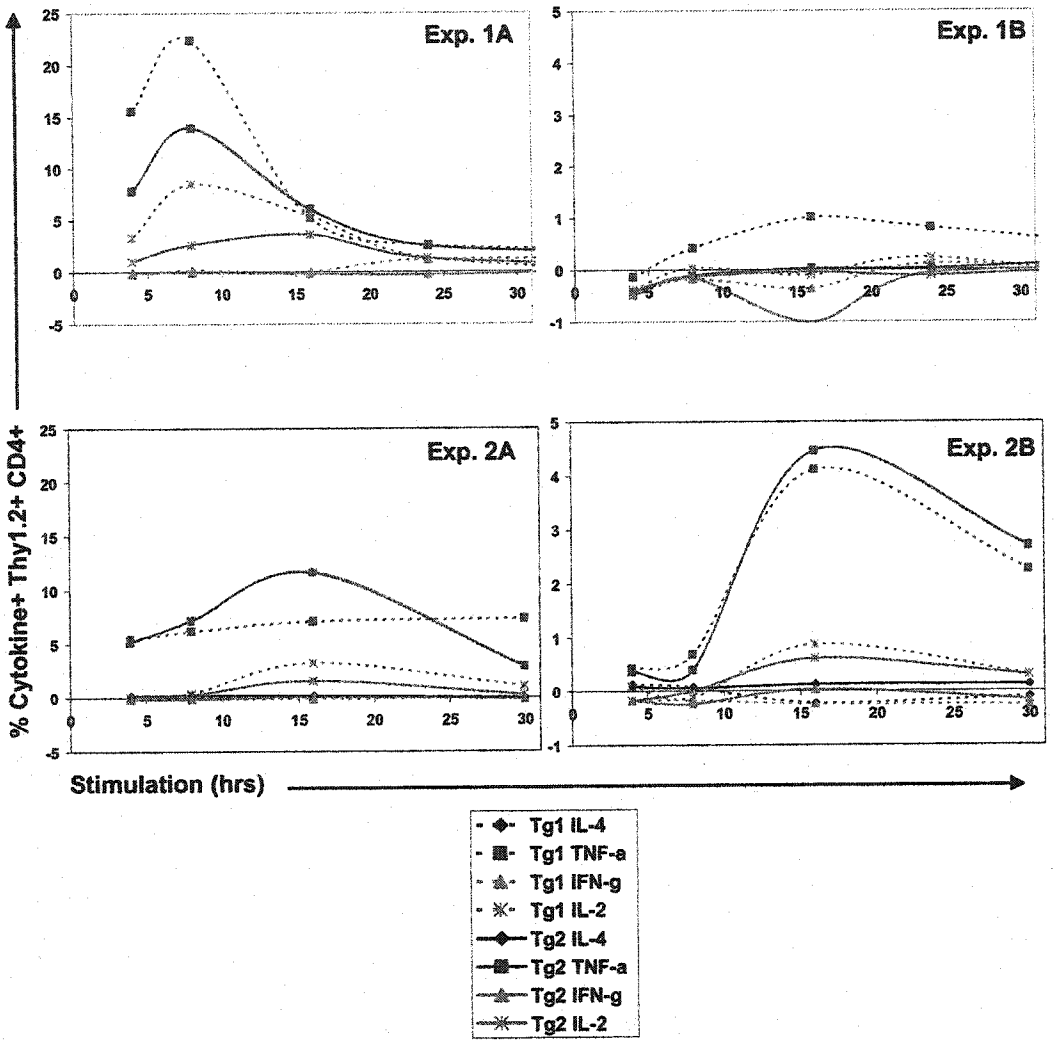

Figure 15. Cytokine production time course by naïve Tg1 and Tg2 T cells stimulated with MBP or MBPAc1-11. Two different experiments (top vs. bottom; Exp. 1 and Exp. 2) using negatively purified Tg1 or Tg2 T cells stimulated with MBPAc1-11 (left panels) or whole MBP (right panels) are shown. T cells were pooled from two Tg1 and two Tg2 mice in Exp. 1 and four Tg1 and five Tg2 mice in Exp. 2. T cells ($1x10^5$) were incubated with ~$9x10^5$ irradiated Thy1.1$^+$ syngeneic APCs and either 10 μM MBPAc1-11 or 21 μg/mL MBP in Exp.1 or 105 μg/mL MBP in Exp. 2. After the indicated stimulation time, cells were surface stained with anti-Thy1.2 and anti-CD4 antibodies, followed by staining for intracellular cytokines. Golgi-stop/plug was present in wells for the last 8 hrs of the stimulation. Antibodies used in Exp. 1 were anti-thy1.2-FITC, CD4-Cychrome, and PE labeled anti-IFN-γ, IL-2 and TNF-α. In Exp. 2 anti- Thy1.2-FITC, CD4-PE Texas Red and PE labeled anti- IFN-γ, IL-2, IL-4 were used as well as anti- TNF-α APC. Cells were double stained for TNF-α and IL-4 in Exp. 2. Data is shown as percent cytokine$^+$ of Thy1.2$^+$CD4$^+$ cells.

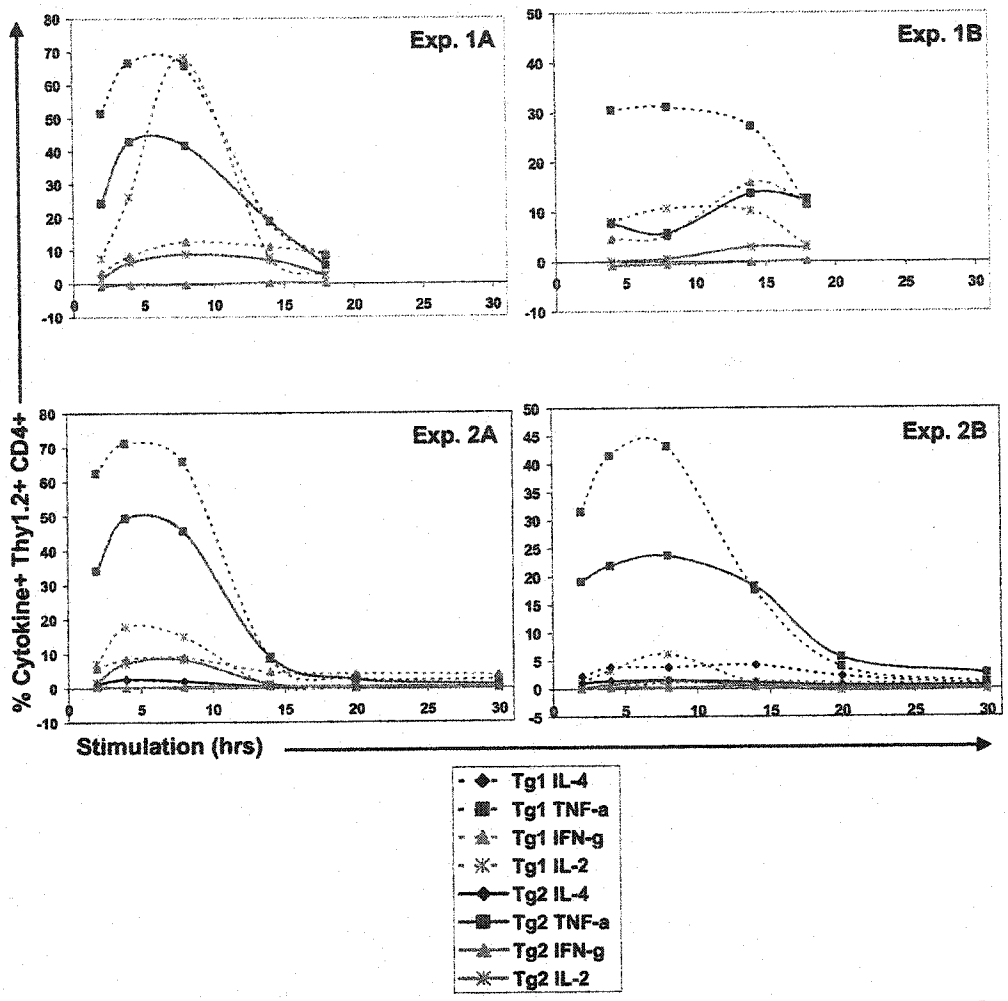

Figure 16. Cytokine production time course by in vitro activated Tg1 and Tg2 T cells stimulated with MBP or MBPAc1-11. Two different experiments (top vs. bottom; Exp. 1 and Exp. 2) using negatively purified Tg1 or Tg2 T cells that had been activated with either 3.2 μM MBPAc1-11 (left panels) or whole MBP (right panels; Exp. 1 T cells were activated with 10.5 μg/mL MBP; Exp. 2, 21 μg/mL MBP) are shown. T cells were pooled from two Tg1 and two Tg2 mice in Exp. 1 and four Tg1 and five Tg2 mice in Exp. 2. T cells ($1x10^5$) were incubated with ~$9x10^5$ irradiated $Thy1.1^+$ syngeneic APCs and either 10 μM MBPAc1-11 or 105 μg/mL MBP. After the indicated stimulation time, cells were surface stained with anti-Thy1.2 and anti-CD4 antibodies, followed by staining for intracellular cytokines. Golgi-stop/plug were in wells for the last 8 hrs of the stimulation. Antibodies used in Exp. 1 were anti-Thy1.2-FITC, CD4-Cychrome, and PE-labeled anti- IFN-γ, IL-2 and TNF-α. In Exp. 2 anti Thy1.2-FITC, CD4-PE Texas Red and PE-labeled anti-IFN-γ, IL-2, IL-4 were used as well as anti-TNF-α APC. Cells were double stained for TNF-α and IL-4 in Exp. 2. Data is shown as percent $cytokine^+$ of $Thy1.2^+CD4^+$ cells.

Naïve and previously activated T cells were analyzed for intracellular cytokines at various time points (ranging from 4-72 hours for naïve cells and 2-24 hours for activated cells) after stimulation with whole MBP or MBPAc1-11 and APCs. Both time courses are shown (Figure 15 and 16). In Experiment 1 we stained intracellularly for TNF-α, IL-2, and IFN-γ and in Experiment 2 we stained for these cytokines as well as IL-4. Also, we increased the concentration of MBP used to generate activated Tg1 and Tg2 T cell cultures two-fold and used five -fold more MBP in the stimulation for cytokine production in Experiment 2 compared to Experiment 1 with the expectation that it would increase cytokine production in T cells.

The most striking observation from these two preliminary experiments was that IFN-γ was detected only in previously activated (stimulated two times) Tg1 T cells and not in activated Tg 2 T cells (Figure 16 and Table 2). Naïve Tg1 or Tg2 T cells did not produce IFN-γ as expected. In MBP-stimulated activated Tg1 cells, IFN-γ was detected in only one of the two experiments (Experiment 1) with maximal cytokine production observed at a later time point (16 hrs) than in MBPAc1-11-stimulated T cells (8 hrs) (Figure 16, top panels, Table 2). Similar percentages of both MBPAc1-11-stimulated Tg1 and Tg2 T cells produced IL-4. MBP-stimulated Tg1 cells produced slightly more IL-4 than Tg2 T cells.

Some additional observations were made with these data. In general, a higher percentage of Tg1 cells were cytokine-positive than Tg2 cells with the exceptions of TNF-α producing naïve Tg2 cells (Figure 15 bottom two panels). In addition, a lower percentage of MBP-stimulated Tg1 and Tg2 cells (naïve or activated stimulations) produced cytokines compared to MBPAc1-11-stimulated cells and, as expected, the percentage of cytokine producing cells was higher in previously activated cells compared to naïve cells (Figure 16, Table 2).

Table 2. Maximum percentage of cytokine-positive MBPAc1-11-specific Tg T cells

	% Cytokine-positive Tg1 T cells[a]				% Cytokine-positive Tg2 T cells[a]			
	Naïve		Activated		Naïve		Activated	
Cytokine	Ac1-11	MBP	Ac1-11	MBP	Ac1-11	MBP	Ac1-11	MBP
IL-4	n.d.[b]/0	n.d./ 0	n.d./ 2	n.d./ 4	n.d./ 0	n.d./ 0	n.d./ 2	n.d./ 1
TNF- α	22/ 7	1/ 4	66/ 71	31/ 43	14/ 12	0/ 4	43/ 49	14/ 24
IFN-γ	1/ 0[c]	0/ 0	12/ 9	16/ 0	0/ 0	0/ 0	0/ 0	0/ 0
IL-2	8/ 3	0/ 0	68/ 18	11/ 6	4/ 2	0/ 0	9/ 8	3/ 1

[a] Maximum percentage of cytokine-positive Tg T cells in Experiment 1 and Experiment 2 (delineated by a slash) are given, respectively.

[b] n.d.= not done

[c] Percentages under 1% are depicted as 0.

Discussion

We analyzed T cell proliferative and cytokine responses as a means to investigate whether Tg1 and Tg2 T cells have differential responses to MBP. These experiments were pursued to investigate the increased susceptibility of the Tg1 versus Tg2 mice to the development of spontaneous EAE. No difference in the proliferative response to either whole MBP or MBPAc1-11 was detected between Tg1 and Tg2 T cells. There was also no difference in proliferative responses to MBPAc1-18, a peptide that is actually processed from whole MBP. It is not clear why purification with anti-Vβ8.2 or anti-CD4 antibodies affects the ability of Tg2 T cells to respond to whole MBP. Positively purified Tg2 T cells maintained their responses to peptide antigens, therefore it is unlikely they are more susceptible to activation-induced cell death. One explanation may be that there are differences in TCR fine specificity or TCR affinity between Tg1 and Tg2 T cells such that interaction of the TCR complex of Tg2 T cells with anti-TCR or anti-CD4 antibodies increases the activation threshold for stimulation with antigen. Blocking of TCR or CD4 molecules on the T cells may inhibit binding to ligand. Alternatively, negative signals

may be delivered to the T cell by cross-linking TCR or CD4. Responses to MBP may be particularly affected because MBP does not stimulate T cells as well as peptide does (for either Tg line), even at the highest concentrations used.

EAE is a primarily inflammatory disease and is initiated in many models by CNS-specific T cells producing inflammatory Th1 cytokines. Increases in anti-inflammatory cytokines such as IL-4, IL-10 and TGF-β in the CNS are associated with recovery from EAE (10). While some evidence suggests that Tg1 T cells produce more inflammatory cytokines and Tg2 cells produce more anti-inflammatory cytokines after stimulation with MBPAc1-11 (117), it was not determined if the cells producing cytokines were actually Tg T cells. Our data are consistent with the idea that Tg2 T cells are, in general, harder to activate and differentiate into Th1-type cells than Tg1 T cells *in vitro*. Lower percentages of both naïve and activated Tg2 cells produced cytokines after stimulation with whole MBP and MBPAc1-11 and activated Tg2 cells did not produce any IFN-γ under the same conditions that allowed a small percentage of Tg1 T cells to produce IFN-γ.

The inconsistencies between these experiments are difficult to reconcile because only two experiments were performed. One source of experimental variation could be due to variation in cytokine production by T cells isolated from different mice. Only 2-3 mice from each Tg line were pooled for each experiment. Differences in cytokine production between MBP-stimulated activated T cells in Experiment 1 versus Experiment 2 could be due to the amount of MBP used to stimulate T cells in each experiment. Higher concentrations of MBP were used in Experiment 2 during the generation of activated T cell cultures and during stimulation for cytokine production. The decrease in cytokine production seen in MBP versus MBPAc1-11-stimulated cultures (for both Tg1 and Tg2 T cells) may be due to unequal molar concentrations of N-termini given to T cells when using whole protein versus peptide or because of toxic effects of the MBP preparation on the T cells.

Strong conclusions from these preliminary data cannot be made due to the inconsistencies between the two experiments, however, even though our *in vitro*

activation protocol was not designed to produce Th1-polarized T cells, IFN-γ production was detected in activated Tg1 T cells in both Experiment 1 and 2 at consistent levels, while IFN-γ was not detected in any Tg2 T cell cultures. *In vivo*, under conditions where spontaneous EAE might develop, environmental stimuli such as exposure to microbial products may polarize Tg T cells to produce Th1 cytokines and Tg1 T cells may be more efficiently polarized under such conditions compared to Tg2 T cells.

Bibliography

1. Whitaker, J. N., and G. W. Mitchell. 1997. Clinical features of Multiple Sclerosis. In *Multiple Sclerosis: Clinical and Pathogenetic Basis*. C. S. Raine, H. McFarland, and W. W. Tourtellotte, eds. Chapman and Hall, London, p. 3.

2. Esiri, M. M., and D. Gay. 1997. The Immunocytochemistry of Multiple Sclerosis Plaques. In *Multiple Sclerosis: Clinical and Pathogenetic Basis*. C. S. Raine, H. F. McFarland, and W. W. Tourtellotte, eds. Chapman and Hall Medical, London, p. 173.

3. McFarland, H. F., R. Martin, and D. E. McFarlin. 1997. Genetic Influences in Multiple Sclerosis. In *Multiple Sclerosis: Clinical and Pathogenetic Basis*. C. S. Raine, H. F. McFarland, and W. W. Tourtellotte, eds. Chapman and Hall Medical, London, p. 205.

4. Martin, R., H. F. McFarland, and D. E. McFarlin. 1992. Immunological aspects of demyelinating diseases. *Annual Review in Immunology 10:153.*

5. Lucchinetti, C., W. Bruck, J. Parisi, B. Scheithauer, M. Rodriguez, and H. Lassmann. 2000. Heterogeneity of multiple sclerosis lesions: implications for the pathogenesis of demyelination. *Annuals of Neurology 47:707.*

6. Lassmann, H., C. S. Raine, J. Antel, and J. W. Prineas. 1998. Immunopathology of multiple sclerosis: report on an international meeting held at the Institute of Neurology of the University of Vienna. *Journal of Neuroimmunology 86:213.*

7. Hemmer, B., S. Cepok, S. Nessler, and N. Sommer. 2002. Pathogenesis of multiple sclerosis: an update on immunology. *15:227.*

8. Zamvil, S. S., and L. Steinman. 1990. The T lymphocyte in experimental allergic encephalomyelitis. *Annual Reviews in Immunology 8:579.*

9. Martin, R., and H. F. McFarland. 1997. Immunology of multiple sclerosis and experimental allergic encephalomyelitis. In *Multiple Sclerosis: Clinical and Pathogenetic Basis*. C. S. Raine, H. F. McFarland, and W. W. Tourtellotte, eds. Chapman and Hall, London, p. 221.

10. Kuchroo, V. K., A. C. Anderson, H. Waldner, M. Munder, E. Bettelli, and L. B. Nicholson. 2002. T cell response in experimental autoimmune encephalomyelitis (EAE): role of self and cross-reactive antigens in shaping, tuning, and regulating the autopathogenic T cell repertoire. *Annu Rev Immunol 20:101.*

11. Iglesias, A., J. Bauer, T. Litzenburger, A. Schubart, and C. Linington. 2001. T- and B-cell responses to myelin oligodendrocyte glycoprotein in experimental autoimmune encephalomyelitis and multiple sclerosis. *Glia 36:220.*

12. Maatta, J. A., M. S. Kaldman, S. Sakoda, A. A. Salmi, and A. E. Hinkkanen. 1998. Encephalitogenicity of myelin-associated oligodendrocytic basic protein and 2',3'-cyclic nucleotide 3'-phosphodiesterase for BALB/c and SJL mice. *Immunology 95:383.*

13. Kaye, J. F., d. R. Kerlero, I. Mendel, S. Flechter, M. Hoffman, I. Yust, and A. Ben Nun. 2000. The central nervous system-specific myelin oligodendrocytic basic protein (MOBP) is encephalitogenic and a potential target antigen in multiple sclerosis (MS). *Journal of Neuroimmunology 102:189.*

14. Holz, A., B. Bielekova, R. Martin, and M. B. Oldstone. 2000. Myelin-associated oligodendrocytic basic protein: identification of an encephalitogenic epitope and association with multiple sclerosis. *Journal of Immunology 164:1103.*

15. Dharmasaroja, P. 2003. Specificity of autoantibodies to epitopes of myelin proteins in multiple sclerosis. *Journal Of The Neurological Sciences 206:7.*

16. de Rosbo, N. K., and A. Ben Nun. 1998. T-cell responses to myelin antigens in multiple sclerosis; relevance of the predominant autoimmune reactivity to myelin oligodendrocyte glycoprotein. *Journal of Autoimmunity 11:287.*

17. Seamons, A., A. Perchellet, and J. Goverman. 2003. Immune Tolerance to Myelin Proteins. *Immunologic Research 28:201.*

18. Campagnoni, A. T., T. M. Pribyl, C. W. Campagnoni, K. Kampf, S. Amur Umarjee, C. F. Landry, V. W. Handley, S. L. Newman, B. Garbay, and K. Kitamura. 1993. Structure and developmental regulation of Golli-mbp, a 105-kilobase gene that encompasses the myelin basic protein gene and is expressed in cells in the oligodendrocyte lineage in the brain. *Journal of Biological Chemistry 268:4930.*

19. Givogri, M. I., E. R. Bongarzone, and A. T. Campagnoni. 2000. New insights on the biology of myelin basic protein gene: the neural- immune connection. *Journal Of Neuroscience Research 59:153.*

20. Lemke, G. 1988. Unwrapping the genes of myelin. *Neuron 1:535.*

21. Privat, A., C. Jacque, J. M. Bourre, P. Dupouey, and N. Baumann. 1979. Absence of the major dense line in myelin of the mutant mouse "shiverer". *Neuroscience Letters 12:107.*

22. Omlin, F. X., H. D. Webster, C. G. Palkovits, and S. R. Cohen. 1982. Immunocytochemical localization of basic protein in major dense line regions of central and peripheral myelin. *Journal Of Cell Biology 95:242.*

23. Martini, R., M. H. Mohajeri, S. Kasper, K. P. Giese, and M. Schachner. 1995. Mice doubly deficient in the genes for P0 and myelin basic protein show that both proteins contribute to the formation of the major dense line in peripheral nerve myelin. *Journal of Neuroscience 15:4488.*

24. Kitamura, K., S. L. Newman, C. W. Campagnoni, J. M. Verdi, T. Mohandas, V. W. Handley, and A. T. Campagnoni. 1990. Expression of a novel transcript of the myelin basic protein gene. *Journal Of Neurochemistry 54:2032.*

25. Mathisen, P. M., S. Pease, J. Garvey, L. Hood, and C. Readhead. 1993. Identification of an embryonic isoform of myelin basic protein that is expressed widely in the mouse embryo. *Proceedings Of The National Academy Of Sciences Of The United 90:10125.*

26. Barbarese, E., J. H. Carson, and P. E. Braun. 1978. Accumulation of the four myelin basic proteins in mouse brain during development. *Journal Of Neurochemistry 31:779.*

27. Liu, H., A. J. MacKenzie-Graham, K. Palaszynski, S. Liva, and R. R. Voskuhl. 2001. "Classic" myelin basic proteins are expressed in lymphoid tissue macrophages. *Journal of Neuroimmunology 116:83.*

28. Zelenika, D., B. Grima, and B. Pessac. 1993. A new family of transcripts of the myelin basic protein gene: expression in brain and in immune system. *Journal Of Neurochemistry 60:1574.*

29. Grima, B., D. Zelenika, and B. Pessac. 1992. A novel transcript overlapping the myelin basic protein gene. *Journal Of Neurochemistry 59:2318.*

30. Landry, C. F., J. A. Ellison, T. M. Pribyl, C. Campagnoni, K. Kampf, and A. T. Campagnoni. 1996. Myelin basic protein gene expression in neurons: developmental and regional changes in protein targeting within neuronal nuclei, cell bodies, and processes. *Journal of Neuroscience 16:2452.*

31. Landry, C. F., J. Ellison, E. Skinner, and A. T. Campagnoni. 1997. Golli-MBP proteins mark the earliest stages of fiber extension and terminal arboration in the mouse peripheral nervous system. *Journal Of Neuroscience Research 50:265.*

32. Feng, J. M., A. O. Fernandes, and A. T. Campagnoni. 2002. Golli-myelin basic proteins delineate the nerve distribution of lymphoid organs. *Journal of Neuroimmunology 123:1.*

33. Feng, J. M., I. M. Givogri, E. R. Bongarzone, C. Campagnoni, E. Jacobs, V. W. Handley, V. Schonmann, and A. T. Campagnoni. 2000. Thymocytes express the golli products of the myelin basic protein gene and levels of expression are stage dependent. *Journal of Immunology 165:5443.*

34. Campagnoni, A. T., and R. P. Skoff. 2001. The pathobiology of myelin mutants reveal novel biological functions of the MBP and PLP genes. *Brain Pathology 11:74.*

35. Bryant, P. W., A. M. Lennon-Dumenil, E. Fiebiger, C. Lagaudriere-Gesbert, and H. L. Ploegh. 2002. Proteolysis and antigen presentation by MHC class II molecules. *Advances in Immunology 80:71.*

36. Starr, T. K., S. C. Jameson, and K. A. Hogquist. 2003. Positive and negative selection of T cells. *Annual Reviews in Immunology 21:139.*

37. Hammerling, G. J., G. Schonrich, F. Momburg, N. Auphan, M. Malissen, B. Malissen, A. M. Schmitt-Verhulst, and B. Arnold. 1991. Non-deletional mechanisms of peripheral and central tolerance: studies with transgenic mice with tissue-specific expression of a foreign MHC class I antigen. *Immunological Reviews 122:47.*

38. de Visser, K. E., T. A. Cordaro, H. W. Kessels, F. H. Tirion, T. N. Schumacher, and A. M. Kruisbeek. 2001. Low-avidity self-specific T cells display a pronounced expansion defect that can be overcome by altered peptide ligands. *Journal of Immunology 167:3818.*

39. Bouneaud, C., P. Kourilsky, and P. Bousso. 2000. Impact of negative selection on the T cell repertoire reactive to a self-peptide: a large fraction of T cell clones escapes clonal deletion. *Immunity 13:829.*

40. Liu, G. Y., P. J. Fairchild, R. M. Smith, J. R. Prowle, D. Kioussis, and D. C. Wraith. 1995. Low avidity recognition of self-antigen by T cells permits escape from central tolerance. *Immunity 3:407.*

41. Ohashi, P. S., S. Oehen, K. Buerki, H. Pircher, C. T. Ohashi, B. Odermatt, B. Malissen, R. M. Zinkernagel, and H. Hengartner. 1991. Ablation of "tolerance" and induction of diabetes by virus infection in viral antigen transgenic mice. *Cell 65:305.*

42. Goverman, J., A. Woods, L. Larson, L. P. Weiner, L. Hood, and D. M. Zaller. 1993. Transgenic mice that express a myelin basic protein-specific T cell receptor develop spontaneous autoimmunity. *Cell 72:551.*

43. Kishimoto, H., and J. Sprent. 2001. A defect in central tolerance in NOD mice. *Nat Immunol 2:1025.*

44. Huseby, E. S., B. Sather, P. G. Huseby, and J. Goverman. 2001. Age-dependent T cell tolerance and autoimmunity to myelin basic protein. *Immunity 14:471.*

45. Miller, J. F., C. Kurts, J. Allison, H. Kosaka, F. Carbone, and W. R. Heath. 1998. Induction of peripheral CD8+ T-cell tolerance by cross-presentation of self antigens. *Immunological Reviews 165:267.*

46. Van Parijs, L., and A. K. Abbas. 1998. Homeostasis and self-tolerance in the immune system: turning lymphocytes off. *Science 280:243.*

47. Shevach, E. M. 2000. Regulatory T cells in autoimmmunity. *Annual Reviews in Immunology 18:423.*

48. Walker, L. S., and A. K. Abbas. 2002. The enemy within: keeping self-reactive T cells at bay in the periphery. *2:11.*

49. Williams, K. C., and W. F. Hickey. 1995. Traffic of hematogenous cells through the central nervous system. *202:221.*

50. Wekerle, H., H. Linnington, H. Lassmann, and R. Meyermann. 1986. Cellular immune reactivity within the CNS. *Trends in Neuroscience 9:271.*

51. Hickey, W. F., B. L. Hsu, and H. Kimura. 1991. T-lymphocyte entry into the central nervous system. *Journal of Neuroscience 28:254.*

52. Brabb, T., P. von Dassow, N. Ordonez, B. Schnabel, B. Duke, and J. Goverman. 2000. In situ tolerance within the central nervous system as a mechanism for preventing autoimmunity. *Journal of Experimental Medicine 192:871.*

53. Hickey, W. F. 1999. Leukocyte traffic in the central nervous system: the participants and their roles. *Seminars In Immunology 11:125.*

54. Derbinski, J., A. Schulte, B. Kyewski, and L. Klein. 2001. Promiscuous gene expression in medullary thymic epithelial cells mirrors the peripheral self. *2:1032.*

55. Anderson, A. C., L. B. Nicholson, K. L. Legge, V. Turchin, H. Zaghouani, and V. K. Kuchroo. 2000. High frequency of autoreactive myelin proteolipid protein-

specific T cells in the periphery of naive mice: mechanisms of selection of the self-reactive repertoire. *Journal of Experimental Medicine 191:761.*

56. Klein, L., M. Klugmann, K. A. Nave, V. K. Tuohy, and B. Kyewski. 2000. Shaping of the autoreactive T-cell repertoire by a splice variant of self protein expressed in thymic epithelial cells. *Nature Medicine 6:56.*

57. Zamvil, S., D. J. Mitchell, A. C. Moore, K. Kitamura, L. Steinman, and J. B. Rothbard. 1986. T cell epitope of the autoantigen myelin basic protein that induces encephalomyelitis. *Nature 324:258.*

58. Dupouey, P., C. Jacque, J. M. Bourre, F. Cesselin, A. Privat, and N. Baumann. 1979. Immunochemical studies of myelin basic protein in shiverer mouse devoid of major dense line of myelin. *Neuroscience Letters 12:113.*

59. Kirschner, D. A., and A. L. Ganser. 1980. Compact myelin exists in the absence of basic protein in the shiverer mutant mouse. *Nature 283:207.*

60. Roach, A., N. Takahashi, D. Pravtcheva, F. Ruddle, and L. Hood. 1985. Chromosomal mapping of mouse myelin basic protein gene and structure and transcription of the partially deleted gene in shiverer mutant mice. *Cell 42:149.*

61. Harrington, C. J., A. Paez, T. Hunkapiller, V. Mannikko, T. Brabb, M. Ahearn, C. Beeson, and J. Goverman. 1998. Differential tolerance is induced in T cells recognizing distinct epitopes of myelin basic protein. *Immunity 8:571.*

62. Loftus, C., E. Huseby, P. Gopaul, C. Beeson, and J. Goverman. 1999. Highly cross-reactive T cell responses to myelin basic protein epitopes reveal a nonpredictable form of TCR degeneracy. *Journal of Immunology 162:6451.*

63. Fairchild, P. J., R. Wildgoose, E. Atherton, S. Webb, and D. C. Wraith. 1993. An autoantigenic T cell epitope forms unstable complexes with class II MHC: a novel route for escape from tolerance induction. *5:1151.*

64. Lafaille, J. J., K. Nagashima, M. Katsuki, and S. Tonegawa. 1994. High incidence of spontaneous autoimmune encephalomyelitis in immunodeficient anti-myelin basic protein T cell receptor transgenic mice. *Cell 78:399.*

65. Deftos, M. L., Y. W. He, E. W. Ojala, and M. J. Bevan. 1998. Correlating notch signaling with thymocyte maturation. *Immunity 9:777.*

66. Pear, W. 1996. *Transient transfection methods for preparation of high-titer retroviral supernatants.* John Wiley and Sons, Inc., New York.

67. Haskins, K., R. Kubo, J. White, M. Pigeon, J. Kappler, and P. Marrack. 1983. The major histocompatibility complex-restricted antigen receptor on T cells. I. Isolation with a monoclonal antibody. *Journal of Experimental Medicine 157:1149.*

68. Reinherz, E. L., K. Tan, L. Tang, P. Kern, J. Liu, Y. Xiong, R. E. Hussey, A. Smolyar, B. Hare, R. Zhang, A. Joachimiak, H. C. Chang, G. Wagner, and J. Wang. 1999. The crystal structure of a T cell receptor in complex with peptide and MHC class II. *Science 286:1913.*

69. Martenson, R. E., G. E. Deibler, and M. W. Kies. 1969. Microheterogeneity of guinea pig myelin basic protein. *Journal of Biological Chemistry 244:4261.*

70. Brabb, T., A. W. Goldrath, P. von Dassow, A. Paez, H. D. Liggitt, and J. Goverman. 1997. Triggers of autoimmune disease in a murine T-cell receptor transgenic model for multiple sclerosis. *Journal of Immunology 159:497.*

71. Luckey, C. J., J. A. Marto, M. Partridge, E. Hall, F. M. White, J. D. Lippolis, J. Shabanowitz, D. F. Hunt, and V. H. Engelhard. 2001. Differences in the expression of human class I MHC alleles and their associated peptides in the presence of proteasome inhibitors. *Journal of Immunology 167:1212.*

72. Martin, S. E., J. Shabanowitz, D. F. Hunt, and J. A. Marto. 2000. Subfemtomole MS and MS/MS peptide sequence analysis using nano-HPLC micro-ESI fourier transform ion cyclotron resonance mass spectrometry. *72:4266.*

73. Hennecke, J., and D. C. Wiley. 2001. T cell receptor-MHC interactions up close. *Cell 104:1.*

74. Garcia, K. C., L. Teyton, and I. A. Wilson. 1999. Structural basis of T cell recognition. *Annu Rev Immunol 17:369.*

75. Wang, J. H., and E. L. Reinherz. 2002. Structural basis of T cell recognition of peptides bound to MHC molecules. *Mol Immunol 38:1039.*

76. Bankovich, A. J., and K. C. Garcia. 2003. Not just any T cell receptor will do. *Immunity 18:7.*

77. Sloan-Lancaster, J., and P. M. Allen. 1996. Altered peptide ligand-induced partial T cell activation: molecular mechanisms and role in T cell biology. *Annu Rev Immunol 14:1.*

78. Wucherpfennig, K. W., and J. L. Strominger. 1995. Molecular mimicry in T cell-mediated autoimmunity: viral peptides activate human T cell clones specific for myelin basic protein. *Cell 80:695.*

79. Jacobsen, M., S. Cepok, W. H. Oertel, N. Sommer, and B. Hemmer. 2001. New approaches to dissect degeneracy and specificity in T cell antigen recognition. *J Mol Med 79:358.*

80. Viner, N. J., C. A. Nelson, and E. R. Unanue. 1995. Identification of a major I-Ek-restricted determinant of hen egg lysozyme: limitations of lymph node proliferation studies in defining immunodominance and crypticity. *Proceedings Of The National Academy Of Sciences Of The United 92:2214.*

81. Lovitch, S. B., J. J. Walters, M. L. Gross, and E. R. Unanue. 2003. APCs present A beta(k)-derived peptides that are autoantigenic to type B T cells. *J Immunol 170:4155.*

82. Unanue, E. R. 2002. Perspective on antigen processing and presentation. *Immunological Reviews 185:86.*

83. Deng, H., R. Apple, M. Clare-Salzler, S. Trembleau, D. Mathis, L. Adorini, and E. Sercarz. 1993. Determinant capture as a possible mechanism of protection afforded by major histocompatibility complex class II molecules in autoimmune disease. *Journal of Experimental Medicine 178:1675.*

84. Fairchild, P. J., H. Pope, and D. C. Wraith. 1996. The nature of cryptic epitopes within the self-antigen myelin basic protein. *8:1035.*

85. Sakai, K., S. S. Zamvil, D. J. Mitchell, S. Hodgkinson, J. B. Rothbard, and L. Steinman. 1989. Prevention of experimental encephalomyelitis with peptides that block interaction of T cells with major histocompatibility complex proteins. *Proceedings Of The National Academy Of Sciences Of The United 86:9470.*

86. Peterson, D. A., R. J. DiPaolo, O. Kanagawa, and E. R. Unanue. 1999. Quantitative analysis of the T cell repertoire that escapes negative selection. *Immunity 11:453.*

87. Watts, C. 1997. Capture and processing of exogenous antigens for presentation on MHC molecules. *Annu Rev Immunol 15:821.*

88. Itano, A. A., and M. K. Jenkins. 2003. Antigen presentation to naive CD4 T cells in the lymph node. *Nat Immunol 4:733.*

89. Croft, M. 1994. Activation of naive, memory and effector T cells. *Curr Opin Immunol 6:431.*

90. Shortman, K., and Y. J. Liu. 2002. Mouse and human dendritic cell subtypes. *Nat Rev Immunol 2:151.*

91. He, X. L., C. Radu, J. Sidney, A. Sette, E. S. Ward, and K. C. Garcia. 2002. Structural snapshot of aberrant antigen presentation linked to autoimmunity: the immunodominant epitope of MBP complexed with I-Au. *Immunity 17:83.*

92. Turley, S. J., K. Inaba, W. S. Garrett, M. Ebersold, J. Unternaehrer, R. M. Steinman, and I. Mellman. 2000. Transport of peptide-MHC class II complexes in developing dendritic cells. *Science 288:522.*

93. Itano, A. A., S. J. McSorley, R. L. Reinhardt, B. D. Ehst, E. Ingulli, A. Y. Rudensky, and M. K. Jenkins. 2003. Distinct dendritic cell populations sequentially present antigen to CD4 T cells and stimulate different aspects of cell-mediated immunity. *Immunity 19:47.*

94. Kropshofer, H., A. B. Vogt, G. Moldenhauer, J. Hammer, J. S. Blum, and G. J. Hammerling. 1996. Editing of the HLA-DR-peptide repertoire by HLA-DM. *Embo J 15:6144.*

95. van Ham, S. M., U. Gruneberg, G. Malcherek, I. Broker, A. Melms, and J. Trowsdale. 1996. Human histocompatibility leukocyte antigen (HLA)-DM edits peptides presented by HLA-DR according to their ligand binding motifs. *J Exp Med 184:2019.*

96. Weber, D. A., B. D. Evavold, and P. E. Jensen. 1996. Enhanced dissociation of HLA-DR-bound peptides in the presence of HLA-DM. *Science 274:618.*

97. Wakkach, A., N. Fournier, V. Brun, J. P. Breittmayer, F. Cottrez, and H. Groux. 2003. Characterization of dendritic cells that induce tolerance and T regulatory 1 cell differentiation in vivo. *Immunity 18:605.*

98. Henri, S., D. Vremec, A. Kamath, J. Waithman, S. Williams, C. Benoist, K. Burnham, S. Saeland, E. Handman, and K. Shortman. 2001. The dendritic cell populations of mouse lymph nodes. *J Immunol 167:741.*

99. Anjuere, F., P. Martin, I. Ferrero, M. L. Fraga, G. M. del Hoyo, N. Wright, and C. Ardavin. 1999. Definition of dendritic cell subpopulations present in the spleen, Peyer's patches, lymph nodes, and skin of the mouse. *Blood 93:590.*

100. Pooley, J. L., W. R. Heath, and K. Shortman. 2001. Cutting edge: intravenous soluble antigen is presented to CD4 T cells by CD8- dendritic cells, but cross-presented to CD8 T cells by CD8+ dendritic cells. *J Immunol 166:5327.*

101. Valdez, Y., W. Mah, M. M. Winslow, L. Xu, P. Ling, and S. E. Townsend. 2002. Major histocompatibility complex class II presentation of cell-associated antigen is mediated by CD8alpha+ dendritic cells in vivo. *J Exp Med 195:683.*

102. Iyoda, T., S. Shimoyama, K. Liu, Y. Omatsu, Y. Akiyama, Y. Maeda, K. Takahara, R. M. Steinman, and K. Inaba. 2002. The CD8+ dendritic cell subset selectively endocytoses dying cells in culture and in vivo. *J Exp Med 195:1289.*

103. Scheinecker, C., R. McHugh, E. M. Shevach, and R. N. Germain. 2002. Constitutive presentation of a natural tissue autoantigen exclusively by dendritic cells in the draining lymph node. *J Exp Med 196:1079.*

104. Hugues, S., E. Mougneau, W. Ferlin, D. Jeske, P. Hofman, D. Homann, L. Beaudoin, C. Schrike, M. Von Herrath, A. Lehuen, and N. Glaichenhaus. 2002. Tolerance to islet antigens and prevention from diabetes induced by limited apoptosis of pancreatic beta cells. *Immunity 16:169.*

105. Kushnir, N., L. Liu, and G. G. MacPherson. 1998. Dendritic cells and resting B cells form clusters in vitro and in vivo: T cell independence, partial LFA-1 dependence, and regulation by cross-linking surface molecules. *J Immunol 160:1774.*

106. Wykes, M., A. Pombo, C. Jenkins, and G. G. MacPherson. 1998. Dendritic cells interact directly with naive B lymphocytes to transfer antigen and initiate class switching in a primary T-dependent response. *J Immunol 161:1313.*

107. Honey, K., and A. Y. Rudensky. 2003. Lysosomal cysteine proteases regulate antigen presentation. *Nat Rev Immunol 3:472.*

108. Hsieh, C. S., P. deRoos, K. Honey, C. Beers, and A. Y. Rudensky. 2002. A role for cathepsin L and cathepsin S in peptide generation for MHC class II presentation. *J Immunol 168:2618.*

109. Pluger, E. B., M. Boes, C. Alfonso, C. J. Schroter, H. Kalbacher, H. L. Ploegh, and C. Driessen. 2002. Specific role for cathepsin S in the generation of antigenic peptides in vivo. *Eur J Immunol 32:467.*

110. DiPaolo, R. J., and E. R. Unanue. 2002. Cutting edge: chemical dominance does not relate to immunodominance: studies of the CD4+ T cell response to a model antigen. *J Immunol 169:1.*

111. Wolf, S. D., B. N. Dittel, F. Hardardottir, and C. A. Janeway, Jr. 1996. Experimental autoimmune encephalomyelitis induction in genetically B cell-deficient mice. *J Exp Med 184:2271.*

112. Hjelmstrom, P., A. E. Juedes, J. Fjell, and N. H. Ruddle. 1998. B-cell-deficient mice develop experimental allergic encephalomyelitis with demyelination after myelin oligodendrocyte glycoprotein sensitization. *Journal of Immunology 161:4480.*

113. Saoudi, A., S. Simmonds, I. Huitinga, and D. Mason. 1995. Prevention of experimental allergic encephalomyelitis in rats by targeting autoantigen to B cells: evidence that the protective mechanism depends on changes in the cytokine response and migratory properties of the autoantigen-specific T cells. *J Exp Med 182:335.*

114. Cross, A. H., J. L. Trotter, and J. Lyons. 2001. B cells and antibodies in CNS demyelinating disease. *J Neuroimmunol 112:1.*

115. Goverman, J. 1999. Tolerance and autoimmunity in TCR transgenic mice specific for myelin basic protein. *Immunological Reviews 169:147.*

116. Song, F., R. M. Wardrop, I. E. Gienapp, S. S. Stuckman, J. Goverman, and C. C. Whitacre. 2002. Differences between two strains of myelin basic protein (MBP) TCR transgenic mice: implications for tolerance induction. *J Autoimmun 18:27.*

117. Song, F., I. E. Gienapp, X. Wang, and C. C. Whitacre. 2002. Activation of Vbeta8 T cells affects spontaneous EAE in MBP TCR transgenic mice. *J Neuroimmunol 123:112.*

118. Laouar, Y., and I. N. Crispe. 2000. Functional flexibility in T cells: independent regulation of CD4+ T cell proliferation and effector function in vivo. *Immunity 13:291.*

Curriculum Vita

Audrey Seamons

Education

1998, Bachelor of Science in Applied Biology-Microbial Biotechnology Emphasis, Utah State University

2004, Doctor of Philosophy in Molecular Biotechnology, University of Washington

Publications

Seamons, A., A. Perchellet and J. Goverman. 2003. Immune Tolerance to Myelin Proteins. *Immunologic Research* 28(3):201-221.

Seamons A., J. Sutton, D. Bai, E. Baird, N. Bonn, B.F.C. Kafsack, J. Shabanowitz, D.F. Hunt, C. Beeson, J. Goverman. 2003. Competition between two MHC binding registers in a single peptide processed from whole myelin basic protein influences tolerance and susceptibility to autoimmunity. *Journal of Experimental Medicine* 197(10):1391-1397.

Cockett N.E., T. L. Shay, J. E. Beever, D. Nielsen, J. Albretsen, M. Georges, K. Peterson, **A. Stephens**, W. Vernon, O. Timofeevskaia, S. South, J. Mork, A. Macuilis, T. D. Bunch. 1999. Localization of the locus causing Spider Lamb Syndrome to the distal end of ovine Chromosome 6. *Mammalian Genome* 10:35-38.